INSTITUTO POLITÉCNICO DE LISBOA

ESCOLA SUPERIOR DE TECNOLOGIA DA SAÚDE DE LISBOA

Brain Connectivity Analysis of Patients with Parkinson's Disease

TIAGO FILIPE SERRANO CONSTANTINO

ADVISOR:

Hugo Alexandre Ferreira, PhD, Institute of Biophysics and Biomedical Engineering, Faculty of Sciences of the University of Lisbon, Lisbon, Portugal

Master in Radiations Applied to Health Technologies

Magnetic Resonance Imaging

Lisbon, 2016

INSTITUTO POLITÉCNICO DE LISBOA

ESCOLA SUPERIOR DE TECNOLOGIA DA SAÚDE DE LISBOA

Brain Connectivity Analysis of Patients with Parkinson's Disease

TIAGO FILIPE SERRANO CONSTANTINO

ADVISOR:

Hugo Alexandre Ferreira, PhD, Institute of Biophysics and Biomedical Engineering, Faculty of Sciences of the University of Lisbon, Lisbon, Portugal

EXAMINING COMMITTEE:

Luís Freire, PhD, Lisbon School of Health Technology, Polytechnic Institute of Lisbon, Lisbon, Portugal

Alexandre Andrade, PhD, Institute of Biophysics and Biomedical Engineering, Faculty of Sciences of the University of Lisbon, Lisbon, Portugal

Master in Radiations Applied to Health Technologies

Magnetic Resonance Imaging

(esta versão incluiu as críticas e sugestões feitas pelo júri)

Lisbon, 2016

Acknowledgments

This dissertation is the result of dedication and continuous effort and could not have been undertaken without the support of many members of my family and friends. Firstly, I would like to thank my advisor, Professor Doctor Hugo Alexandre Ferreira, for the opportunity, self-determination and support he has provided. I am sure, with the guidance he has given me, that I am ready to continue my long journey in this wonderful field. I would also like to thank André Santos Ribeiro and Ricardo Maximiano for their time, effort and advice. Their sincere interest and passion for the search of knowledge will always stay with me as exciting and motivating pathways.

I would like to thank Professor Ana Luisa Vieira, Ph.D for her patience, friendship and clear advice.

I would like to express my gratitude to Doctor Marianne Braunschweig and Renato Leuenberger from the Hospital Centre of Biel in Switzerland for granting me the opportunity to achieve this new and important academic degree.

I must mention, and express my appreciation to, some of my friends who have always supported me. I would like to thank Francisco Conceição, Helena Martins and João Francisco for all the support they gave me when I was in Lisbon and for always being thre for me. Thank you also to Guilherme Teixeira, Renato Santos, João Nuno, Hugo Falcato and Sérgio Inácio for their resilience and companionship.

I also need to thank two of my colleagues and friends who have helped me with their friendship, Dr. Ingo Holler and Dr. Sasha Berger, Ph.D.

I would like to express my sincere gratitude to my friend, IT engineer Telmo Gonçalves, for his patience and assistance.

I would like to thank two other people who represent everything I am right now, my grandmother Emilia Serrano and my lovely cousin Lita Pedrosa. They have shown me what love and respect are.

I want to thank my parents for their trust and support and my brother and his family for their friendship as well.

Lastly, I am indebted to my lovely fiancée, Ana Resendes, for all her love, help and understanding.

Resumo

Atualmente existe um debate sobre *"Scans Without Evidence for Dopaminergic Deficit"* (*SWEDD*) de ser uma patologia independente ou um subtipo benigno da doença de Parkinson (DP).

Neste estudo analisou-se a conectividade estrutural cerebral de 30 indivíduos saudáveis, 29 doentes com *SWEDD* e 29 doentes com DP, utilizando diversos *softwares* especializados e a teoria dos grafos para caracterizar 96 regiões de interesse. Diferentes métricas de imagem e de conectividade foram obtidas a partir de dados de imagem em ponderação T1 e de tensor de difusão.

Em relação aos dados demográficos dos grupos, observaram-se diferenças estatísticas na *Unified Parkinson Disease Rating Scale* entre os indivíduos saudáveis (Controlo) e os doentes com DP (p = 0,000), e com SWEDD (p = 0,000). Na comparação Controlo *vs* DP, várias diferenças foram observadas em relação às métricas de imagem e de conectividade, particularmente nos núcleos da base de ambos os hemisférios. No Controlo *vs SWEDD*, as regiões dos lobos frontal e parietal mostraram alterações nas métricas de conectividade, particularmente o giro marginal superior e o giro parietal superior de ambos os hemisférios. Na DP *vs SWEDD*, foram observadas alterações de métricas de imagem e de conectividade, particularmente no polo frontal e no córtex pré-frontal anterior. Todos os resultados observados neste estudo estão de acordo com a literatura sobre mudanças observadas nas regiões relacionadas com as, mesolímbica mesocortical e nigroestriatal. Estes achados sugerem que o estudo da conectividade estrutural é um importante método para distinguir *SWEDD* e DP.

Palavras-chave: Conectividade estrutural cerebral, Doença de Parkinson, Ressonância Magnética, Imagem por Tensor de Difusão, Imagem Ponderada em T1.

Abstract

Currently, there is an ongoing controversy about Scans Without Evidence of Dopaminergic deficit (SWEDD) being a Parkinson's Disease (PD) lookalike disease or a benign subtype of PD.

In this study the brain structural connectivity of 30 healthy subjects, 29 patients with SWEDD and 29 patients with PD was analysed, using various specialized software and graph theory to characterize the structural connectivity of 96 regions of interest. Different imaging metrics and connectivities were obtained from diffusion tensor imaging and T1 weighted data.

With regard to group data, statistical differences in Unified Parkinson Disease Rating Scale (UPDRS) scores were observed between healthy subjects (Control) and PD ($p=0.000$) and SWEDD ($p=0.000$) patients. In comparing Control vs PD, several differences were observed regarding various imaging and connectivity metrics, particularly in the basal ganglia of both hemispheres. In comparing Control vs SWEDD, regions of the frontal and parietal lobes showed various connectivity metrics changes, particularly in the superior marginal gyrus and superior parietal gyrus of both hemispheres. In comparing SWEDD vs PD, various DTI-based imaging and connectivity metrics changes were observed, particularly in the frontal pole and rostral middle frontal gyrus.

All results observed in this study are in agreement with the literature regarding observed changes in regions related to the nigrostriatal, mesocortical and mesolimbic pathways. These findings suggest that the study of SC is an important method in distinguishing between SWEDD and PD.

Keywords: Structural Connectivity, Parkinson's Disease, Magnetic Resonance Imaging, T1-w, Diffusion Tensor Imaging.

Contents

List of tables

List of Figures

List of Abbreviations

ACP – Anatomical connectivity probability

ACS – Anatomical connectivity strength

ADC – Apparent Diffusion Coefficient

aMRI – Anatomical Magnetic Resonance Imaging

BCT – Brain Connectivity Toolbox

CAr – Cortical Area

ClusC – Clustering Coefficient

CThk – Cortical Thickness

CVol – Cortical Volume

DaT – Dopamine Transporter

Deg – Node degree

DICOM – Digital Imaging and Communications in Medicine

Dist – Distance

DKI – Diffusion Kurtosis Imaging

dMRI – Diffusion Magnetic Resonance Imaging

DSI – Diffusion Spectrum Imaging

DTI – Diffusion Tensor Imaging

DWI – Diffusion Weight Imaging

Edge Betw – Edge Betweenness

FA – Fractional Anisotropy

FACT – Fibre Assignment by Continuous Tracking

FACTID – FACT including Diagonals

FiberConn – Fibre Connections

fMRI – Functional Magnetic Resonance Imaging

FSL – FMRIB Software Library

GM – Grey Matter

HARDI – High Angular Resolution Diffusion Imaging

IBM – International Business Machines

L – Lambda

MATLAB – Matrix Laboratory

MD – Median Diffusion

MDS – Movement Disorder Society

MIBCA – Multimodal Imaging Brain Connectivity Analysis

MP-Rage – Magnetization Prepared Rapid Acquisition Gradient Echo

MRI – Magnetic Resonance Imaging

NIFTI – Neuroimaging Informatics Technology Initiative

PET – Positron Emission Tomography

PPMI – Parkinson’s Progression Markers Initiative

RGB – Red Green Blue

ROI – Region of Interest

SD – Spherical Deconvolution

SN – Substantia Nigra

SNc – Substantia Nigra compacta

SNr – Substantia Nigra reticulata

SPM – Statistical Parametric Mapping

SPSS – Statistical Package for the Social Sciences

SWEDD – Scans without evidence for dopaminergic deficit

T1-w – T1 weighted

UPDRS – Unified Parkinson’s Disease Rating Scale

WM – White Matter

1. Introduction

Since the twentieth century we have been witnessing the development of artificial neural networks, which, inspired by their biological counterparts, are enabling us to gain a deeper understanding of the workings of the brain. (1,2) Today, it is believed that the basis of information processing and mental representations lies in neural networks.

Understanding the brain's structural and functional organization is a daunting task, as described already in the first studies on the brain and most notably since the mid 1990s when the complexity of the macroscopic behaviour of a system of interacting elements that combines statistics and arbitrariness with constancy became clear.(1–3)

The increasing accessibility and manageability of large and high-quality data sets on an extensive range of neural structures has led to an essential vision: different neural systems often share certain important values, which can be quantitatively considered and categorised by the same parameters.(2,3) In other words, we can see similarities in many complex organizations despite the complexity and differences in the details or their connections.

In recent years, many scientific studies have been performed using small-world architectures.(2–4) This mathematical model has been used on brain networks in humans and other animals, and over a varied range of measures in space and time, to understand the structural and functional systems.(2–4)

One of the most common neurodegenerative diseases and the most common form of Parkinsonism is Parkinson's disease (PD).(5–7) This disease usually affects people over 50 years old. Usually, the manifestations of this disease are seen at the level of the gait and tremors (at this stage the patient has important impairments of the dopaminergic system).(6,8) Many studies have been conducted with a view to developing diagnostics and understanding the mechanism of this disease. One of the methods is neuroimaging, such as magnetic resonance imaging with the diffusion-weighted imaging (DWI) technique. This technique has been used for accessing the microstructure of the regions with parameter changes in diffusion parametric and connectivity levels.(8,9)

The principal motivation for carrying out this research is to demonstrate the importance of the study of structural brain connectivity in patients with PD,

particularly by evaluating the differences in the structural brain connectivity between patients with PD, those with SWEDD and healthy individuals. A multimodal approach was adopted and graph theoretical analysis performed to demonstrate the potential of this method for studying the networks of the brain.

In this thesis, the T1-weighted (T1-w) and DTI capabilities of the fully automated all-in-one connectivity analysis toolbox Multimodal Imaging Brain Connectivity Analysis (MIBCA) were exploited. The software performs preprocessing, connectivity and graph theory analysis, and visualization of multimodal data such as anatomical MRI (aMRI), diffusion MRI (dMRI), functional MRI (fMRI) and positron emission tomography (PET). Here, MIBCA was applied to SWEDD and PD patients.

The thesis is organized as follows:

1. Theoretical concepts
2. Materials and methods
3. Results and discussion
4. Limitations of this study
5. Conclusions.

2. Theoretical concepts

2.1 Parkinson’s Disease – Definition and diagnostic

Since the detection and conception of the first definition of PD, there have been huge changes in the conceptualization of the disease.(5,6) One of the reasons is a better understanding of motor manifestations,(5) clear pathological definitions (6,7) and the availability of therapy that is as effective as a part of the diagnostic criteria.(7,9) In addition, our knowledge about this pathology has always been under constant development: for example, the identification of non-motor aspects, recognition of neurodegeneration symptoms and a better understanding of genetics and environmental factors.(6,7) With these improvements, clinicians and specialists in genetics, epidemiology, pathology and basic science have created their own definitions of disease,(5,7) all of them valid, but none representing the “truth”.(8)

The International Parkinson and Movement Disorder Society (MDS) has created one “standard” definition.(8) Most clinicians would approve of the notion that this disease is diagnosed through a combination of clinical and pathological syndromes.(7,8) However, until now, the “real” definition of PD has not fully emerged.(9)

PD is a neurodegenerative disease and the most common neurodegenerative cause of Parkinsonism (a combination of bradykinesia, rigidity and tremor).(5,6,8) It is considered a hallmark within the severe loss of dopaminergic projection neurons of the substantia nigra (SN).(6–8) Normally, this neurodegeneration consequence involves a loss of dopaminergic innervation in the striatum and is frequently accompanied by extensive extranigral pathology.(7,8) PD is more prevalent in subjects of advanced age, with the average age for onset of the disease being over 50 years.(6)

The aetiology is still unknown. However, it is known that there are environmental factors such as exposure to toxins that are associated with increased genetic predisposition of the individual and can promote the expression of this disease.(7–9) It can also occur as a result of many mutations in genes that are associated with the disease’s development.(7,8)

The SN is divided anatomically and functionally into two distinct areas/regions.(9,10) The first region is the SN pars compacta (SNc) and is characterized by neuron projections to the globus pallidus, striatum, subthalamic nucleus, anterior thalamic nuclei and prefrontal cortex.(10) The second SN region is the SN pars reticulata

(SNr) and this region involves neuron projections to the ventral thalamic nuclei and prefrontal cortex and receives afferents from the striatum, external globus pallidus and subthalamic nucleus.(10)

The damage to the SN is not uniform. Usually, this degeneration occurs in the caudal and lateral SN and the caudolateral sensorimotor putamen.(8,9) In PD, the motor symptoms appear as a consequence of preferential degeneration in the sensorimotor region.(7–9)

Beyond the motor symptoms, this neurodegenerative pathology causes variable degrees of cognitive impairment in a high fraction of patients.(6,8) The occurrence of cognitive deficits in untreated, newly diagnosed patients has been described to be between 19 and 24 %.(6,7) The most commonly affected cognitive functions are attention/executive, episodic memory, visuospatial/visuoperceptual and hallucinations.(8,9) A higher risk exists of subsequently developing dementia in patients with mild cognitive impairment.(6,8) It is critical as well to mention that this pathology normally involves the whole brain.(9)

2.1. Anatomy of the brain in Parkinson’s disease’

Anatomical structures undergo many alterations in PD, starting in the brainstem, following with subcortical regions and finishing in the cortex.(7,8) In this thesis it will be demonstrated and explained where the most common regions for such changes are in a subject with this pathology.

- Mesencephalon: Regions that belong to the brainstem, located above and below the bulge of the diencephalon.(10)

These regions are formed by nucleus ruber, which is responsible for the regulation and unconscious control of motor activity (this region is the most important area in patients with PD), and the SN, which is responsible for keeping muscle tone and coordination activities. Both belong to the dopaminergic system.(10)

- Basal ganglia (Figure 2.1): Also known as the striate nucleus, this is the collection of GM in the cerebrum including the corpus striatum, amygdala and claustrum.(10)

A large group of nuclei at the base of the cerebral cortex controls movement and coordination and affects involuntary movements.(10) It has meaningful connections with other regions of the brain, specifically the thalamus, subthalamic nuclei, red

nuclei and substantia nigra.(10) The basal ganglia include the caudate nucleus, putamen, globus pallidus, subthalamic nucleus, nucleus accumbens and substantia nigra.(10)

In PD, there is a loss of dopaminergic innervation to the dorsal striatum and a cascade of consequences.(10) The putamen is responsible for regulating larger movements and exercises effects on various types of knowledge.(10) The caudate nucleus influences knowledge and memory, and is responsible for voluntary movements.(10) Lastly, the nucleus accumbens is related to mechanisms of pleasure and motivation.(10)

Another important structure in the brain, specifically in patients with PD, is the thalamus.(10) Located between the cortex and the mesencephalon,(10) it is responsible for mood and movements associated with anger and fear. It is an important region of the central nervous system because nearly all brain nerves pass through (except the olfactory nerve).(10)

At the subcortical level the hippocampus should be noted. This region belongs to the limbic system and has a role to play in the consolidation of information from short-term and long-term memory, navigation, learning and emotion.(10)

Lastly, the motor cortex is responsible for, and involved in, control, planning and execution mechanisms as well as voluntary movements.(10) It is located in the frontal lobe and includes three regions: the primary motor cortex (precentral gyrus), the premotor cortex (lying within the frontal lobe just anterior to the primary motor cortex – Brodmann area 6) and supplementary motor area (located in the midline surface of the hemisphere just in front of the primary motor cortex).(10)

In addition, it is important to mention other regions of the cortex, such as the association cortex, responsible for ensuring that the movements are adaptive to the requirements of the organism and social context.(10) This region is compounded of the prefrontal and the parietal cortex.(10)

Three routes of dissemination are identified: the nigrostriatal, mesolimbic and mesocortical pathways.(10)

The first one starts in neurons of SNc and ends in the striatum.(10) It is associated with the transmission of information. Alterations in the dopaminergic system can result in information loss. This also occurs in the primary motor cortex.(10)

The mesolimbic pathway is also known as the “reward pathway” in the brain.(10) This pathway is also associated with the dopaminergic pathway.(10) It has projections to the nucleus accumbens, amygdala, olfactory nucleus, hippocampus and medial prefrontal cortex.(10)

Lastly, the mesocortical pathway is a dopaminergic pathway that joins the ventral tegmentum to the cerebral cortex (in the frontal lobes).(10)

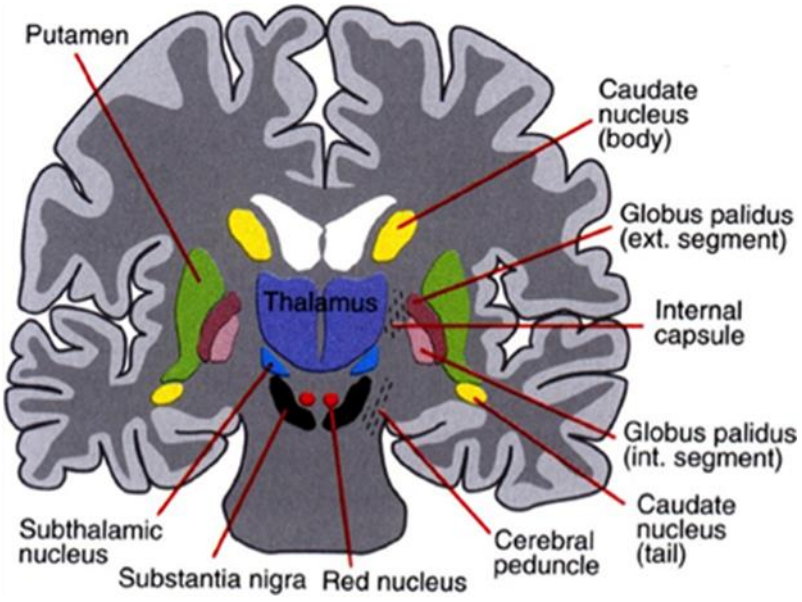

Figure 2.1 – Illustration of basal ganglia and their components. The basal ganglia include the subthalamic nucleus and substantia nigra whose component structures are highly interconnected.(10)

2.1.2 Scans Without Evidence of Dopaminergic Deficit Disease

Scans Without Evidence of Dopaminergic Deficit (SWEDD) is the term created to refer to a group of patients that mystify this movement disorder through the absence of an imaging abnormality in those that have clinical, or are presumed to have, PD.(11) The acronym SWEDD does not offer any aetiological evidence; it has usually been used in the medical literature and clinical practice as a diagnostic label.(12,13) While many authors until now have said that this pathology is independent of PD, others have suggested that it can be a subtype of PD.(12,14) This kind of medical controversy has been studied to clarify what it represents.(12) Several studies involving patients with this term have been carried out and the results reflect that while most SWEDD cases are due to a clinical misdiagnosis of PD, there is a small quantity of patients with SWEDD that may have a subtype of

PD.(12–14) The continuing significance of this discussion has, as a consequence, led one of the largest observational organizations in patients with PD, the PPMI (http://www.ppmi-info.org/), to include patients with SWEDD.(12)

With regard to the clinical follow-up of patients diagnosed with SWEDD, they are generally unresponsive to dopaminergic medication, adding to a non-existence of clinical progression, and preservation of olfactory function (usually compromised in PD).(11,14) Many studies discovered that dopamine deficiency did not develop constantly, nor did subjects improve their hypermetabolism in the basal ganglia, with hypometabolism in the parietal cortex (particularly the premotor and posterior regions) being typical of PD.(11,14) Since 2013, several studies have described that SWEDD patients might have dystonic tremor.(11) However, clinical findings were related to three groups. Specifically, true fatigability and decrement, re-emergent tremor on variation in posture and the presence of non-motor irregularities facilitated a diagnosis of PD.(11,14) It is also important to mention that a lack of true bradykinesia, head tremor and dystonia was more indicative of SWEDD.(13) Additionally, another study demonstrated enhanced facilitation and loss of spatial specificity typical of dystonia in a subsection of SWEDD patients.(13,14)

Repeated clinical studies revealed that SWEDD patients may have a better prognosis than PD and this may be advantageous for the quality of life of the patients.(11,14)

Clinical evaluation with constant examinations every several months can help to clarify the difference between PD and SWEDD and there should be no need to start symptomatic therapy.(14) However, to achieve early diagnosis and differentiation between the two diseases, a neuroprotective therapy should be available.(14) When the clinical examinations are still unclear, neuroimaging (functional imaging) could be a second criterion.(13,14)

Lastly, many studies revealed that one-half of the SWEDD patients had a positive familial history compared to only 1/6 of the PD patients.(13,14) Once again, neuroimaging could be useful and advantageous in differentiating between pathologies.(13)

It is important to mention also that the UPDRS is used to follow the longitudinal course of Parkinson's and SWEDD diseases. The UPDRS is a scale that was developed in an effort to provide a comprehensive, efficient and flexible means to monitor PD-related incapacity and impairment. Normally, the scale has four

components, largely derived from previous scales that were modified by a group of specialists in PD (Part I, Mentation, Behaviour and Mood; Part II, Activities of Daily Living; Part III, Motor; Part IV, Complications).

Table 2.1 summarizes the differences between PD and SWEDD.

Table 2.1 – Clinical differences between PD and SWEDD

	Features
PD	Responsive to dopaminergic medication, clinical progression and affection of olfactory function.
SWEDD	Unresponsive to dopaminergic medication, non-existence of clinical progression, preservation of olfactory function, lack of true bradykinesia, head tremor and dystonia.

2.2 Diffusion Weight Imaging and its principles

Brownian motion is characterized by the consequence of a random microscopic motion of diffusion molecules, also called “diffusion phenomena”.(15,16) This effect reflects the movement or stagnation of every molecule or particle in a fluid, which is also thermal molecular energy.(15)

Particles in a free medium have a random direction and change all the time (random walk).(15,16) When the concentration has a stable situation, diffusion can be defined mathematically, or otherwise statistically, when the situation is unstable and the diffusion can be observed and measured (resulting in macroscopic flux of the fluid).(16)

The diffusion phenomena respect a Gaussian distribution (with a zero mean) and the variance is proportional to time:

$$< r^2 > = 2\,NDt \qquad (1)$$

where $< r^2 >$ is the mean square displacement and N (for MRI measurement purposes, this value is one) is the “dimensionality” of the space in which diffusions are measured.(15,16) D is the diffusion coefficient and defines the movement of particles in a fluid at a certain temperature (D has molecular size and temperature dependency, and the environment that it is inserted in is also an important factor).(15,16) The methods executed in diffusion-weighted imaging (DWI) measure (indirectly) the shifts of the molecules in one dimension.(15,17)

By exploring the natural sensitivity of MRI to motion, it is possible to measure diffusion *in vivo*. In MRI, we see different phase shifts in accumulative spins (this accumulation occurs due to natural Brownian motion), resulting in a lower MR signal intensity.(17)

In a clinical situation, these properties are small, and extremely difficult to measure and study, but we can increase sensitivity to motion using higher field gradient pulses in a pulse sequence.(16) The simplest pulse sequence in MRI consists of a spin–echo sequence with two extra gradient pulses placed around the refocusing pulse (Figure 2.1).(16) During the first gradient pulse, spins sitting at one specific Larmor frequency in different positions on the magnet bore are shown as different magnetic fields.(17) However, they accumulate different phase alterations.(15,17) It is also important to point out that when the spins stay immobile, the phase accumulated during the second gradient pulse is identical to the phase accumulated during the first gradient pulse since the first phase shift is reversed by the 180º pulse, and the net phase shift is zero.(15) What happens to a group of diffusing spins moving arbitrarily? The result consists in spins not having the same gradient field during the two pulses.(16,17) When needed to acquire the echo time (TE), the phase shifts will be arbitrarily dispersed, resulting in an imperfect refocusing of the sequence and signal attenuation.(16) This attenuation will have a positive correlation

with D.(16)

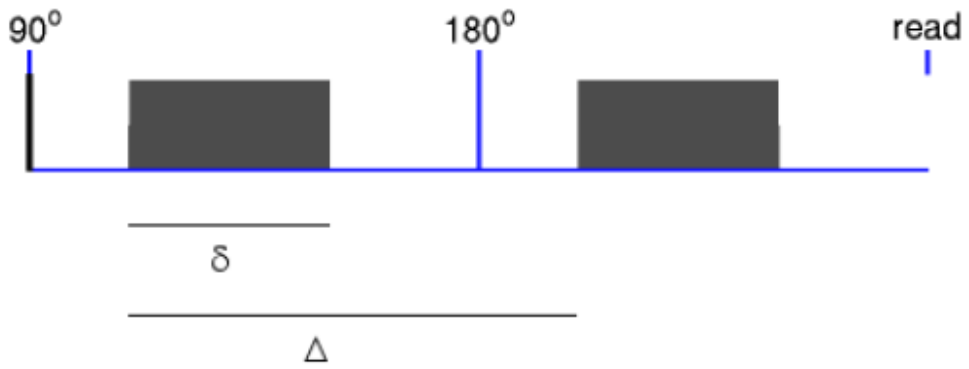

Figure 2.2 – Illustration of application of two diffusion gradients.(17)

What do isotropy and anisotropy state mean? The first definition is when the human body does not have any barrier to the motion of spins;(16,18) however, the second has a different behaviour. In other words, it is once we have alteration in Brownian motion (for example, the axonal fibres provoke a low mean diffusivity), changing the molecular direction in a certain path (normally, the molecules have a perpendicular direction when they do not have any obstacle, however with barriers to motion the molecules will have a parallel path).(17,18)

Due to the influence of the motion of spins, a gradient with a certain intensity (G) and length (L) is applied, which will provoke a spin phase shift in each voxel.(16,18) After a TE/2 time, a 180º RF pulse is applied, which is responsible for the inversion of the phase of the spins. After a timed interval, following the start of the first gradient, a second gradient is applied that causes refocusing of spins.(16,17) However, the spins will retain a residual gap allowing the quantification of the diffusion that occurs.(15,17)

When the diffusion gradients and their sensitization effect on molecules are mentioned, it is important to take into account the arrangement of the sequence. Thus, the signal to obtain, for a voxel of tissue in which molecular diffusion occurs, is equal to the intensity of a T2-weighted image, i.e. equal to that which would be obtained if the diffusion gradients were not applied with a decrease due to the reduction of signal resulting from the loss of coherence associated with the displacement suffered by molecules.(15,17)

The expression giving the measured signal intensity is:

$$S = S_0 e^{-bD} \quad (2)$$

where S_0 is the signal intensity without DWI and b is a factor that reflects the strength and timing of the gradients used to generate DWI images.(17)

When a longer time is considered there will be a higher molecular shift, which causes greater attenuation in the weighted signal diffusion.(16,17) Gradients with larger amplitude and duration are in turn responsible for contrast enhancement in the signal, by inducing a higher shift phase in molecules that are subject to the diffusion process.(15,17) However, if ADC maps are considered, areas of higher intensity correspond to regions of higher diffusivity, because this method is sensitive to the diffusion length.(17) To estimate the ADC, we need to obtain at least two images, corresponding to different b values.(17,18)

In 1985, clinicians applied the use of one new sequence, echo-planar imaging (EPI).(15,16) The main aim of this sequence was to reduce the acquisition time.(17,18) The basic principles of this sequence are nearly identical to those of the spin echo, however the newest sequence needs just one excitation pulse, which is why the sequence is also called “diffusion-weighted single-shot echo-planar imaging” (DW-SS-EPI) (Figure 2.3).(16) As previously mentioned, the greatest improvement was the reduced acquisition time due to the capacity of the system to acquire in “just” one time repetition (TR). However, as a consequence, this sequence has a low signal-to-noise ratio (SNR) and is prone to high artefacts.(16) These artefacts are duo to spatial fluctuations in magnetic susceptibility.(17,19)

Other sequences have been developed, such as EPI-Multi-Shot (Figure 2.4), where the k-space is obtained with several TRs,(17) resulting in the reduction of the effective time between the echoes.(17) As a consequence, this sequence increases the acquisition time, but on the other hand, we have better SNR and resolution and fewer artefacts.(16,17)

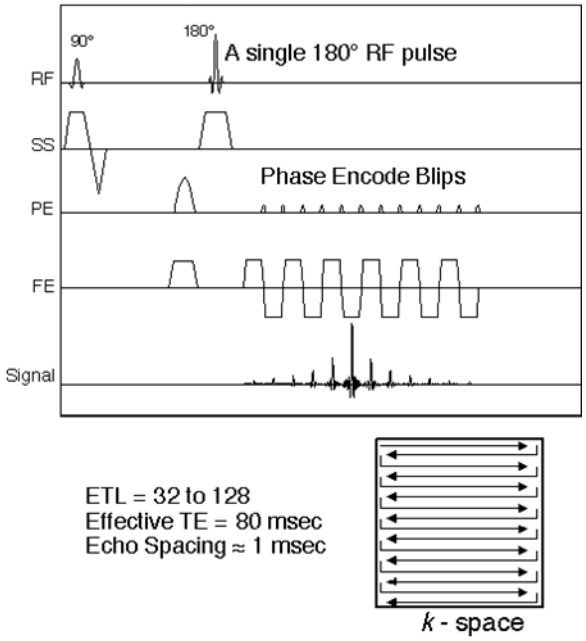

Figure 2.3 – Illustration of EPI single-shot sequence.(16) ETL= echo train length.

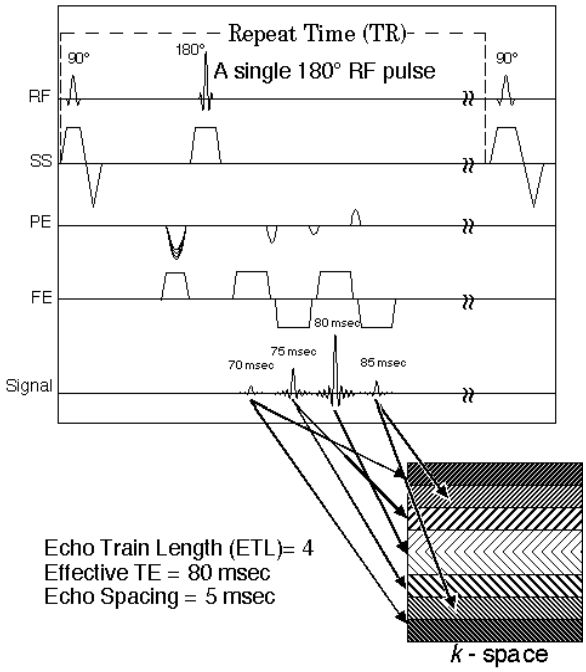

Figure 2.4 – Illustration of EPI multi-shot sequence.(16)

2.2.1 Diffusion Tensor Imaging

DWI is an MRI technique that is defined by the application of magnetic field gradient pulses to study water diffusion.(17,18) Water diffusion is the main basis of DWI and refers to the arbitrary translational motion of molecules.(15) Normally, diffusion gradients are applied along the three axes (x,y,z) of the scanner.(16,17) DWI

enables the acquisition of the trace and mean diffusivity (MD). The mathematical formula(18) for calculating the trace is:

$$Tr(D) = Dxx + Dyy + Dzz \quad (3)$$

where Dxx, Dyy and Dyy are coefficients along the x, y and z axes.

The MD is defined as:

$$MD = \frac{Dxx + Dyy + Dzz}{3} = \frac{Tr(D)}{3} \quad (4)$$

Diffusion tensor imaging (DTI) involves the application of diffusion gradients in at least six directions.(17,18) This technique offers other indices with the orientation of diffusion and the central path of diffusivities. However, to improve this technique, the acquisition of more than six directions is recommended.(18) Anisotropy is the directional dependence of diffusion, which defines the spatial variations of water molecular shifts (Figure 9).(18,19) Anisotropy is defined by the fractional anisotropy (FA) parameter and demonstrates the presence of oriented structures such as axons in fibre bundles. FA is characterized by:

$$FA = \sqrt{\frac{1}{2}}.\sqrt{\frac{(\lambda_1 - <\lambda>)^2 + (\lambda_2 - <\lambda>)^2 + (\lambda_3 - <\lambda>)^2}{(\lambda_1) + (\lambda_2) + (\lambda_3)}} \quad (5)$$

where λ_1, λ_2 and λ_3 are the eigenvalues of each diffusion direction. The central path of diffusion and the direction perpendicular to it are calculated by the spatial alignment of these components.(19,20)

Another important scalar function or invariant that can be identified from the diffusion eigenvalues is relative anisotropy (RA).(17) This function is given by:

$$RA = \sqrt{\frac{3}{2}}.\sqrt{\frac{(\lambda_1 - <\lambda>)^2 + (\lambda_2 - <\lambda>)^2 + (\lambda_3 - <\lambda>)^2}{(\lambda_1)^2 + (\lambda_2)^2 + (\lambda_3)^2}} \quad (6)$$

DTI was developed to measure the diffusion tensor in each voxel, enabling the estimation of MD values or degrees of anisotropy in each voxel (Figure 2.5). An anisotropic statement is when the value is 1, however when the value is 0 it is isotropic.(17,18) The signal can be obtained by:

$$ln\frac{S}{S_0} = \sum_{i}^{3}\sum_{j}^{3} b_{ij}D_{ij} \quad (7)$$

b_{ij} represents one matrix (17,18) with values b and D_{ij} is the tensor diffusion defined as:

$$D = \begin{bmatrix} D_{xx} & D_{xy} & D_{xz} \\ D_{yx} & D_{yy} & D_{yz} \\ D_{zx} & D_{zy} & D_{zz} \end{bmatrix} \quad (8)$$

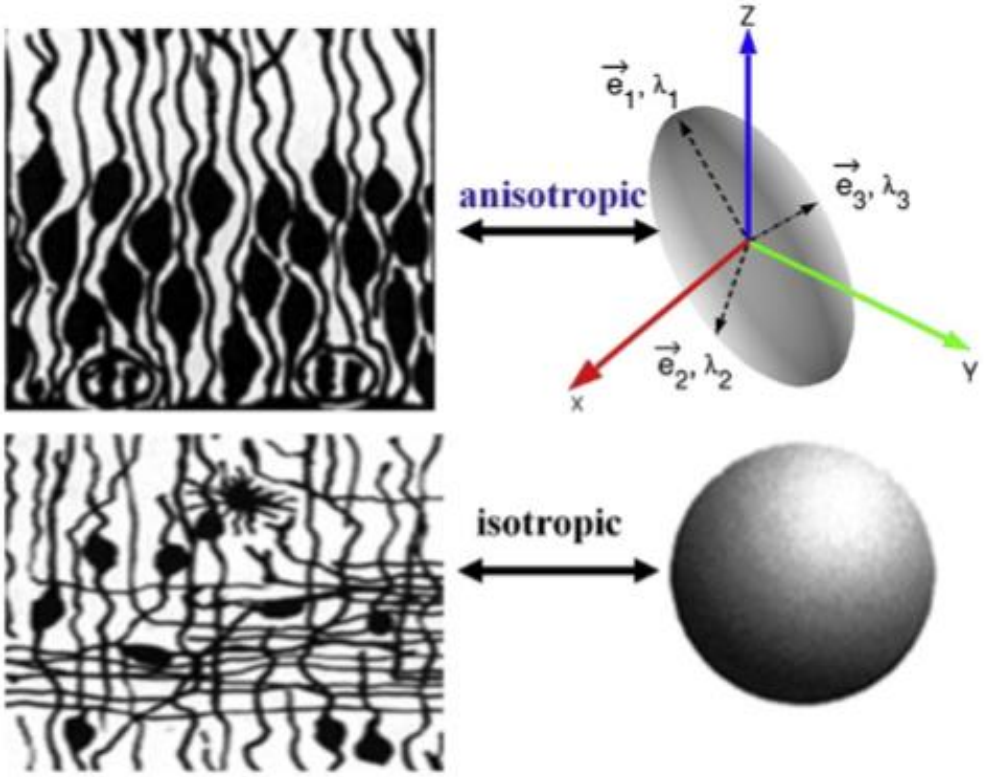

Figure 2.5 – Illustration of anisotropic (up) and isotropic (down) direction with the ellipsoid demonstration of the single tensor model.(17)

Diffusion directions (Figure 2.4) are represented by eigenvectors oriented along the main direction of diffusion (e1, axial or even parallel) and perpendicular to it (e2 and e3, radial or perpendicular) and by their respective diffusivities, or eigenvalues.(17,21) Anisotropy is still a process that is not completely defined and understood.(17,21) It reflects the organization in bundles of fibres running in parallel.(17,18) It is usually recognized that variations in transverse diffusivity mostly reflect transversal loss,(21) but alterations in radial diffusivity (RD) can express myelin damage.(17,22)

FA and RA both have a numerator variance associated with three eigenvalues. These two scalar functions allow the mean ADC (apparent diffusion coefficient) along the three orthogonal axes to be calculated. It is also normal to generate a colour map (RGB system – red, green and blue) where the intensity is given by the value of FA (Figure 2.6).(18) This system allows a more direct view of “neural” directions (blue corresponds to superior-inferior, red diffusion in the lateral-medial axis, and the green component diffusion according to the anterior-posterior axis).(17,21)

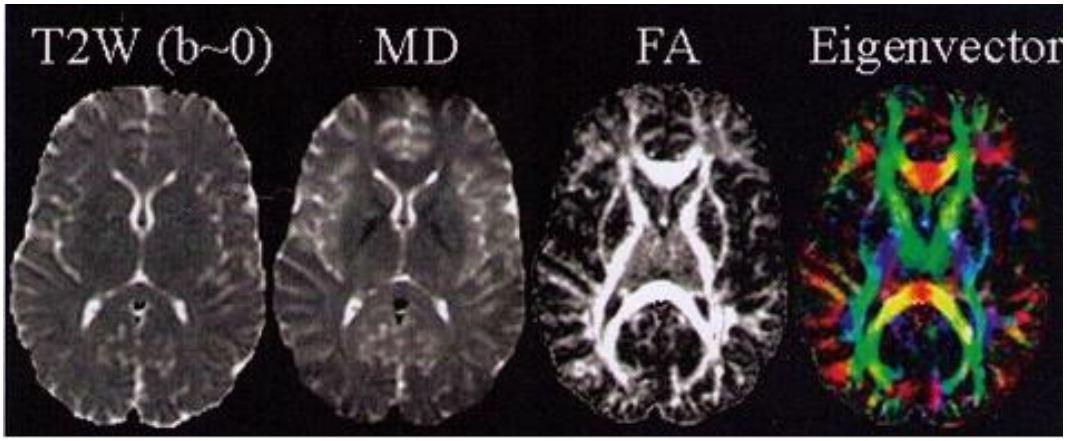

Figure 2.6 – Quantitative maps of DTI measurements. Left to right: T2-weighted reference image (i.e. b=0 s/mm^2), the mean diffusivity (MD), fractional anisotropy (FA; hyperintense in white matter), the major eigenvector direction indicated by RGB colour map (red: right-left; green: anterior-posterior; blue: superior inferior).(22)

2.2.2 Tractography and its algorithms

Tractography is the only currently existing tool capable of identifying and measuring existing anatomical connections in the human brain *in vivo*, in a non-invasive way.(21,22) This technique enables identification and characterization of the nervous system that would otherwise only be possible using more conventional and invasive methods, such as axonal tracing using injected radioisotopes.(20,22)

Instead of using the RGB system to visualize the orientation of major eigenvectors, tractography enables the 3D visualization of white matter connections (anatomy and connectivity between numerous regions).(18,20)

In tractography three vital fibres exist and they are nominated throughout their location and according to their connections (Figure 2.7). They are:

- **Association Fibres** – These fibres connect regions inside the same hemisphere, with anterior-posterior direction.(21)
- **Projection Fibres** – They are responsible for the signal transmission between the cortical and subcortical regions in a superior-inferior direction.(21)
- **Commissural Fibres** – Establish the edge between both hemispheres.(21)

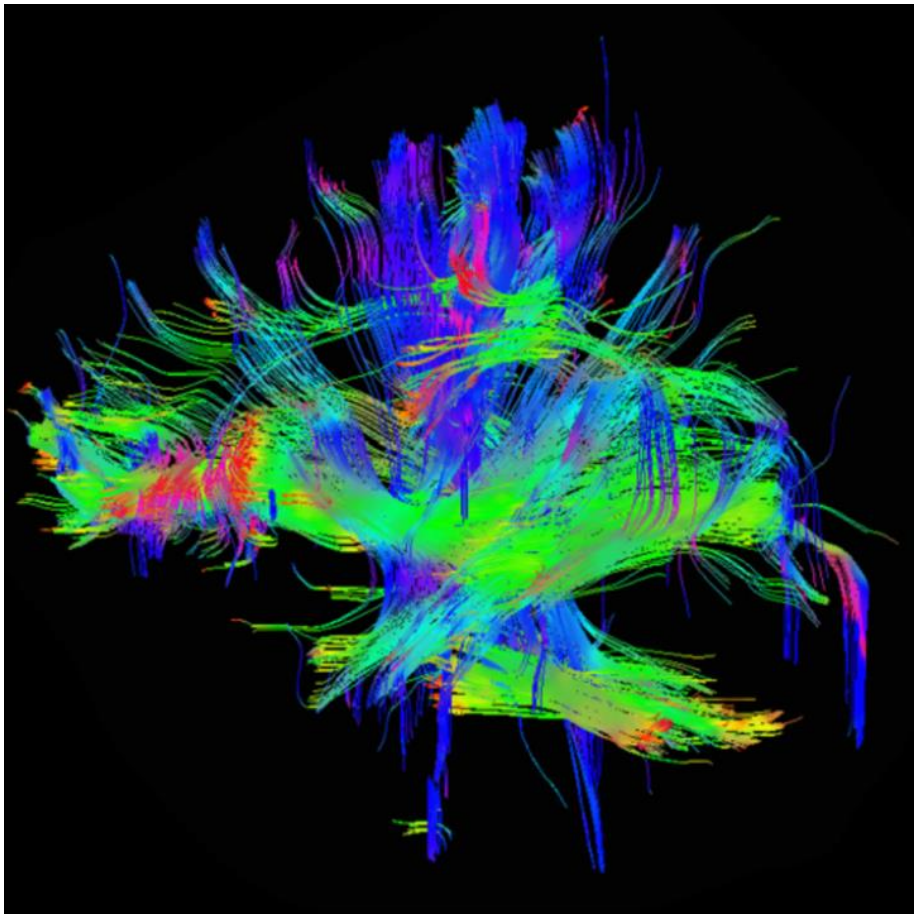

Figure 2.7 – White matter fibre tracts seen with DTI Tractography (256 diffusion directions).(18)

The principal aim of this method is to reconstruct the direction of neuron bundles in the brain of patients undergoing MR-DTI.(17,21) This tool can detect the main direction of water movement in the brain thought to coincide with the behaviour of neuronal WM as a result of its deterministic tractography technique and its value as a surgical planning tool.(17,22)

Tractography can normally be generated with two main algorithms: deterministic or probabilistic.(20)

In this work, only the deterministic algorithm is considered. Although the number of voxel connections in the deterministic algorithm is more limited, the reconstructed connections provide higher connectivity values than some of the trajectories reconstructed by probabilistic tractographies.(17,20) This is because the latter method produces a great diversity of paths for the fibres,(17,20) whereas in the former, the fibres tend to follow the same trajectory in most cases, demonstrating the consistency of this algorithm and resulting in higher connectivity values.(17)

It is paramount to mention that all algorithms share the same heuristic rules on the termination of reconstruction.(17,19) Thus, the reconstruction ends for one of two reasons: the front streamline reaches a region where the value of FA is less than a predetermined value (threshold), or if the angle between voxels exceeds a predefined threshold.(20)

If the reader wants more detailed information about reconstruction and propagation algorithms, the reading of *Diffusion MRI: From Quantitative Measurements to In Vivo Neuroanatomy* is recommended.(17)

Deterministic algorithms were the first to be invented and they are the most commonly used in clinical applications.(17) Deterministic algorithms try to discover the path from an original voxel based on the main direction of diffusion in each voxel path, not taking into account the uncertainty related to this approximation.(21,23) The deterministic approach is only able to rebuild a streamline by voxel (a streamline is a curve tangent to the vector field). However, this approach has some limitations, such as the inability to identify fibres branching or take into account the uncertainty in the estimated parameters.(22,23)

The most common examples of deterministic algorithms (Figure 2.8) are Fibre Assignment by Continuous Tracking (FACT) and Fibre Assignment by Continuous Tracking Including Diagonals (FACTID).(22,23)

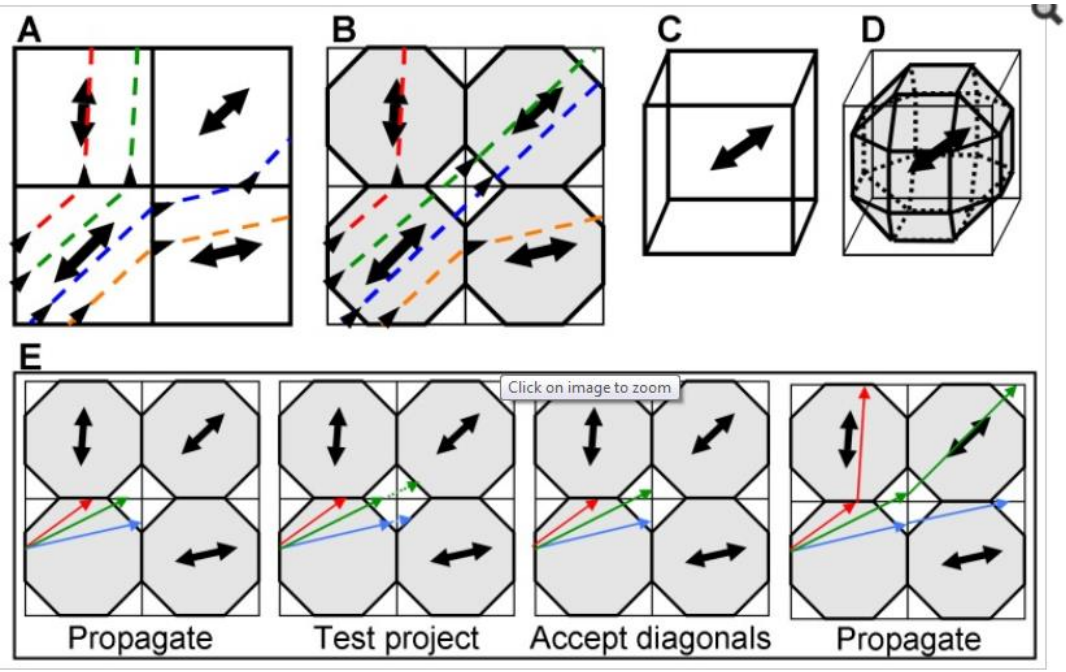

Figure 2.8 – Deterministic algorithms: FACT (top row) permits the propagation streamlines and FACTID (bottom row) enables the propagation diagonally.(23)

The top row of Figure 2.8 and Figure 2.9 demonstrates the explanation of streamline reconstruction with the FACT algorithm using four test tracts (dotted lines, direction of propagation given by small arrowheads) incoming and crossing the bottom-left voxel in the direction of highest diffusion or the upper-right voxel (dual-direction arrow).(21,23) However, the FACT approach does not allow the diagonal path.(23) In other words, the orientation of the axes powerfully disturbs the estimated tracts, producing numerous artefacts (present in the calculations, due to signal noise and to grid dependence).(23) In fact, if the reference was rotated 45º, this propagation could occur.(21,23) Nonetheless, the diagonal orientation of the axes can actually occur and be detected with the FACTID reconstruction algorithm,(23) allowing the possibility of spreading each WM tract for eight voxels of their neighbourhood (2D) or 26 in the case of 3D instead.(21,23) The FACTID shows more tolerance relatively to the orientations of the axes and therefore this approach is also characterized by better SNR than the FACT.(22,23)

DTI has other limitations, such as SNR and low resolution, as well.(21,23) To overcome these limitations and to correct the fibres' orientation heterogeneity in each voxel, other methods and techniques have been developed.(21,22) Examples of these are Q-ball, spherical deconvolution (SD), diffusion spectrum imaging (DSI),

diffusion kurtosis imaging (DKI) and high-angular resolution diffusion imaging (HARDI).(21,22)

The DTI and tractography are a very useful technology that are used to study several questions which the brain connectivity.

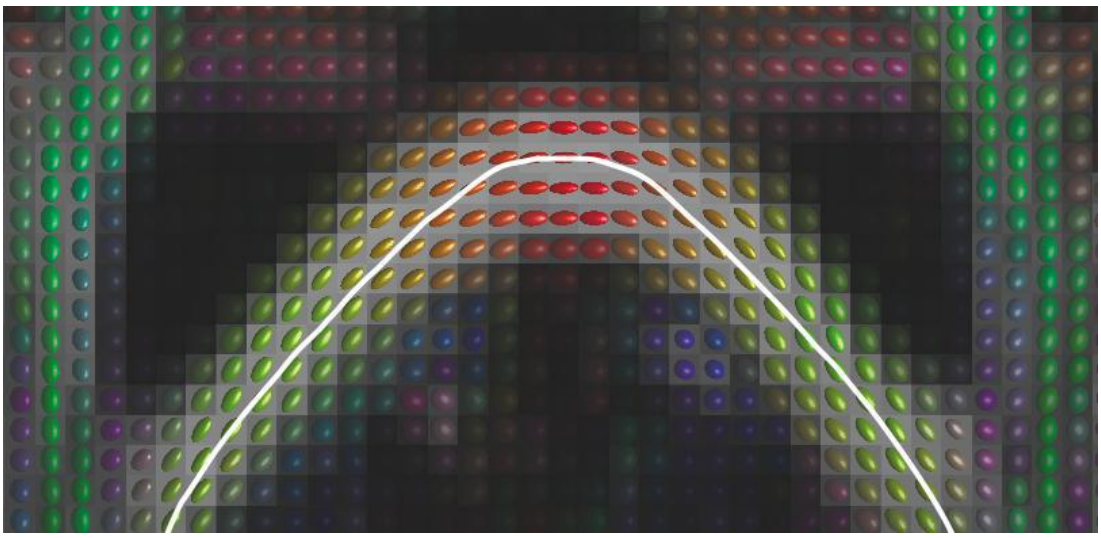

Figure 2.9 – In the deterministic method the principal direction of diffusion is characterized by the axis of diffusion of ellipsoids. The white line represents the streamline obtained after the various regions according to the preferred diffusion direction estimated at each voxel being connected.(23)

2.3 Brain Connectivity

The brain is never idle. Even when resting, a large number of neuronal activities are happening in many areas of our brain.

Brain connectivity has revealed the multifaceted brain organization through innumerable networks (21,24) allowing the segregation and integration of information during high cognitive processes, but also the definition of clinical consequences of alterations encountered in the development of neurological diseases.(21,24)

These complex interactions can be studied by applying imaging methods, which, through anatomical and functional properties of the brain structures, can be measured simultaneously.(21,24) However, most brain imaging studies employ a multivariate functional analysis, where each brain region is studied together with reference to others.(24,25)

The structural or anatomical connectivity defines the white matter networks between brain regions.(21,22) Brain connectivity is usually represented by a binary or weighted network whose topology can be studied using the graph theory.(24,25)

Functional connectivity is defined as statistical dependencies among remote neurophysiological events, which can analyse statistically many regions combining the regions of interest and based on anatomical or structural information that is quantified with measures of statistical dependencies, such as correlations, coherence or transfer entropy.(21,24) However, the associations can arise in a variety of ways.(24,26)

The main problem with functional connectivity analysis is the complexity due to the quantity of links that could be analysed.(27) In other words, the number of combinations always depends on the areas/regions that are involved, making it practically impossible to obtain reliable solutions.(25,27) On the other hand, if analyses of structural connections are performed, then the number of functional networks to be studied can be limited.(25,27)

Finally, the last connectivity method is called the “effective connectivity network”,(25) which measures the influence that one neural system applies over another.(25,27)

To underline the mechanism of anatomical (structural), functional and effective connectivity in the whole brain, the graph theory has demonstrated an important role in this area of study.(27) Below, the fundaments of this mathematical model are explained.

2.4 Graph theory – The Fundaments

Over the past 20 years neuroscience has become one of the most important areas of study and scientific research, especially neuroimaging. In recent years,(25,28) an exponential increase of research in human neural networks – connectivity brain systems – has been seen.(25,28)

A network (or a graph) is a mathematical model that involves a group of nodes (or vertices) and connections (or edges) between pairs of nodes.(28) This group of nodes and connections is an abstract model that can be used to characterize the different levels of the brain systems.(28) An edge can represent functional or structural connections between the cortical and subcortical nodes, if based on data analysis of human neuroimaging.(2,28) Once the brain connectivity matrix is

constructed, its properties and topologies can be quantified by a variety of measures that have been recently developed in the field of statistical physics of complex networks and graph theory.(2,25)

All connections explain the network properties of each graph. Figure 2.10 represents two types of network model, where the simplest case (unweighted undirected networks) assumes that each connection has the same strength or length and the edges are bidirectional (meaning that the information can travel between the edge from A to B node and/or vice versa).(28) It is also important to point out that in unweighted networks, edges are absent (0) or present (1).(25,28) The second network case is weighted, which means that the edges may differ from each other with different strengths,(28) or some physical distance between the connected vertices.(2) Each connection with a different strength or length represents one precise weight.(25,28) Lastly, a network could be directed if its links are unidirectional (the information travels just in one way or direction).(24,28) Normally graphs can be graphically described by plotting the nodes and edges(24,28) according to their estimated measures(24,28) but the most valuable format for representing networks is their matrix form.(25,28)

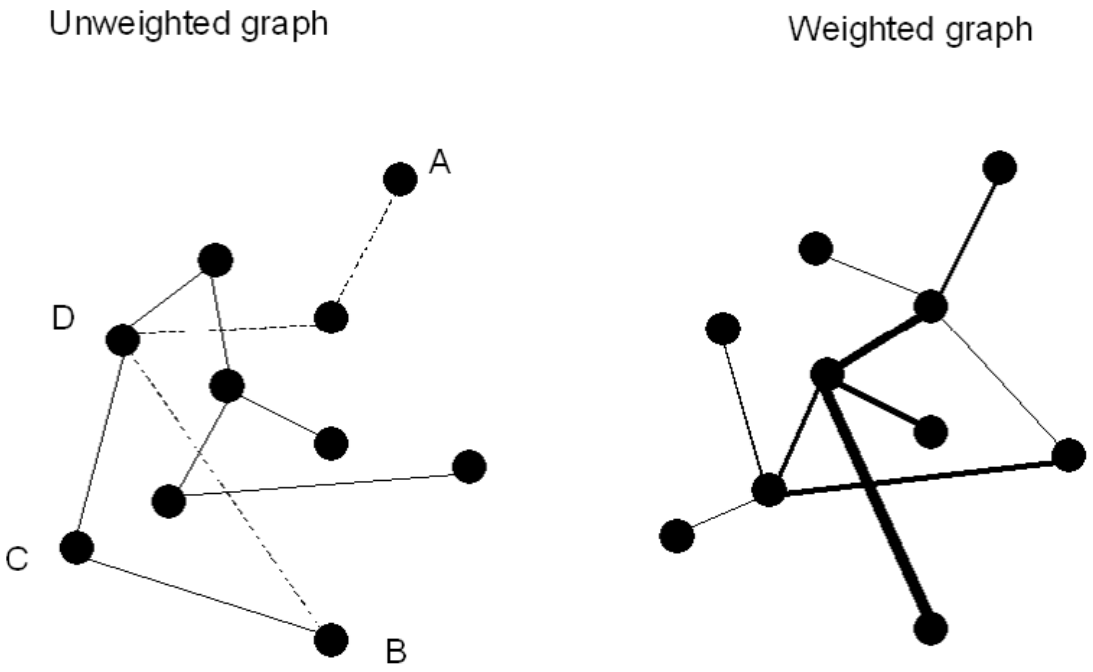

Figure 2.10 – Unweighted graph (left) and Weighted graph (right). In the Unweighted graph each connection has the same strength or length and the edges are bidirectional. In the Weighted graph the edges may differ from each other with different strengths, or some physical distance between the connected vertices.(28)

2.4.1 Network measures and types

The precise quantification of network metrics is the most significant advantage of theoretical network analysis, because it enables the diagnostics of network topology and efficiency.(22,24)

There is a quantity of measures that can describe quantitatively a network. In this section, the most significant measures and types of networks are described.

Node (or vertex): This is the basic element in the graph theory (28) where node v represents an intersection point of a graph.(24,28)

Edge (connections or links): This is the link between two nodes or vertices (Figure 2.10)(24) where the edge $e_{i,j}$ represents the initial extremity, for example i, and the terminal point, j.(24)

Degree: This is one of the most basic and important measures and is often represented by k.(21,28) The degree is the number of edges within a specific node.(24,28) The degree of distribution gives the probability that a randomly chosen node will have degree k.(28) The shape of the degree distribution provides information about the structure of the graph.(22,28) As described above, different types of graphs have their individual typical degree distribution (Figure 2.11).

Clustering coefficient (ClusC): Clustering is an important property in social networks. It is defined as the probability of the degree to which two random node neighbours are connected to each other.(21,28) The ClusC of a vertex can have values of between 0 and 1.(24) The ClusC c_i of node i with degree k_i can be defined as the ratio of the actual number of links between neighbours of i, i.e. m and i (e_i), to the maximum possible number of links between those neighbours (neighbours of i are nodes directly connected to node i).(24) When good interconnection exists between the neighbours we have high clustering coefficients.(24) This suggests a better protection against the loss of an individual node (little impact on the structure of the network).(24,28)

$$c_i = \frac{2e_i}{k_i\,(k_i - 1)} = \frac{\sum_{j,m} a_{i,j}{}^{a}{}_{j,m}{}^{a}{}_{m,i}}{k_i\,(k_i - 1)} \qquad (9)$$

where a is the edges between nodes.

Characteristic path length or lambda (L): The characteristic path length L of a network is the average distance between all pairs of nodes.(22,28) The path length or distance $d_{i,j}$ between two nodes i and j is the smallest number of links that can connect i to j.(28) For an undirected graph of N nodes, the mean path length is: (24,28)

$$L = \frac{1}{N(N-1)} \sum_{i,j \in N, i \neq j} d_{i,j} \tag{10}$$

Distance matrix (Dist): This is a two-dimensional matrix that covers the distances, taken pairwise, between nodes.(4,28) In a weighted graph, the distance between two vertices can be defined as the minimum of the sums of the weights on the shortest paths joining the two vertices.(4)

Assortativity: This is the correlation between the properties of the nodes linked directly by a path. Theoretically, the graph is assortative if vertices with a high degree tend to be linked to other vertices with a high degree, and vertices with a low degree are linked to other lowdegree vertices (positive degree correlation).(4,28) On the other hand, a disassortative graph is represented by a negative degree correlation.(4,28) The average degree knn of the neighbours of a node with degree k is given by:

$$k_{nn}(k) = \sum_{k'} k' P\,(k'|k) \tag{11}$$

where $P\,(k'|k)$ is the conditional probability that a path of node degree k´ points to a node with degree k. Most of the technological and biological networks tend to be disassortative, whereas the social networks tend to be assortative.(24,28)

Betweenness centrality (betw): This is the index of the relative relevance of a node or edge.(22,24) In other words, this is the number of shortest paths that a node or edge participate in.(24,28) It is expressed by the equation:

$$b_i = \sum_{j,k \in N, j \neq k} \frac{n_{j,k^{(i)}}}{n_{j,k}} \tag{12}$$

This is the ratio of all the shortest paths between node j and k that are passed through by a path' $i\,(n_{j,k^{(i)}})$.(22,28) Later it is necessary to be divided by all the

shortest paths between nodes j and k $(n_{j,k})$.(22) This mathematical model explains the consequences of the loss of a particular edge or vertex.(28)

Edge Betweenness (Edge Betw): The characterize the fraction of all the shortest paths covering a specific edge,(22,28) meaning that edges with high values of betweenness centrality contribute to a large number of short paths.(22,24)

Local Efficiency: Represents the mean of the efficiencies of all subgraphs of neighbours of each vertex of the graph.(28)

Global Efficiency: This is the inverse of the shortest distance in the network (between vertices).(21,28)

Graph Eccentricity: Represents the maximum length of the shortest path between any nodes.(21,24) The radius of G is the value of the smallest eccentricity.(22,28) The diameter of G is the value of the highest eccentricity.(28)

Hub: This is a nuclear portion in the architecture of the network.(28) It receives all neural synapses and transmits to the others (Figure 2.11).(24,28) Hubs can be distinguished by using many different graph measures;(28) most of them reflect aspects of node centrality.(22,28) The simplest network measure used for classifying hubs is the node degree, also called “degree centrality”, which is equivalent to the number of edges that are preserved by each node.(28)

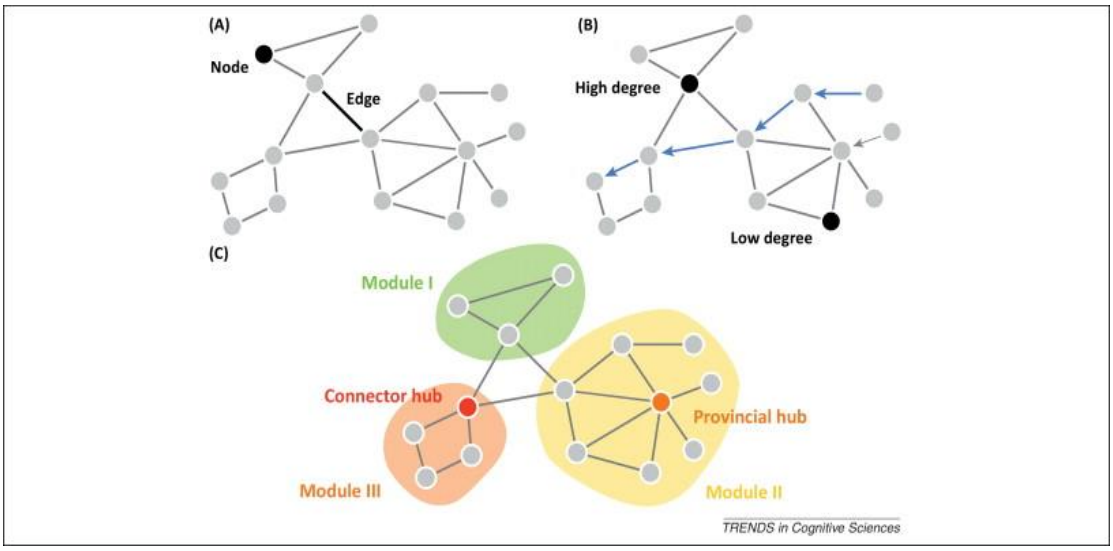

Figure 2.11 – The network’s architecture. (A) Nodes or vertices (describing neurons/brain regions) and edges (represent functional or structural connections between the cortical and subcortical nodes). (B) A path length resembles a sequence of edges that are traversed when travelling between two nodes. Low-degree nodes are nodes that have a low number of edges and high-degree nodes (often referred to as “hubs”) are nodes that have a high number of edges. (C) Numerous Hubs. Connector hubs can

establish connections between modules (high degree). Provincial hubs are high-degree nodes that connect to nodes in the same module.(28)

Vulnerability and dynamic importance: Tries to assess the impact of node (or edge) removal with respect to the global network synchronization or communication by associating graph metrics before and after node (or edge) deletion.(24)

Deg, ClusC and L are core measures of the graph theory network (24,28) and with them, four different types of graph can be extracted. They are described as follows (Figure 2.12).(24,28)

Ordered or lattice-like network: Each node is linked to its k adjacent neighbours.(2,28) The meaning of “adjacent” depends on the dimension considered in which the network is demonstrated.(2,28) If the network is considered with one dimension the theoretical values of ClusC and L are high and large, respectively.(24)

Small-world network (small-worldness): This network refers to the collective of networks in which the mean geodesic or shortest path distance between nodes increases satisfactorily slowly as a function of the number of nodes in the network.(24,28) Can be thought of as a lattice-like network where a small fraction of the edges has been arbitrarily rewired.(24,28) This network has a C close to that of an ordered network, however it has a very small L close to that of a random network.(21,28)

Random network: All links are arbitrarily rewired to pairs of nodes and possess short L and small ClusC values.(21,24)

Scale-free network: A scale-free network is a connected graph with a property of some of the edges originating from a given node exhibiting a power law distribution.(21,28) When nodes are detached from a random network, the connectivity of the random network decays slowly with time until the network reaches a point where it breaks into smaller distinct domains that are unable to connect.(28) On the other hand, scale-free networks resist random failures, because it is statistically unlikely that the strongest connected nodes would fail under random conditions.(25,28)

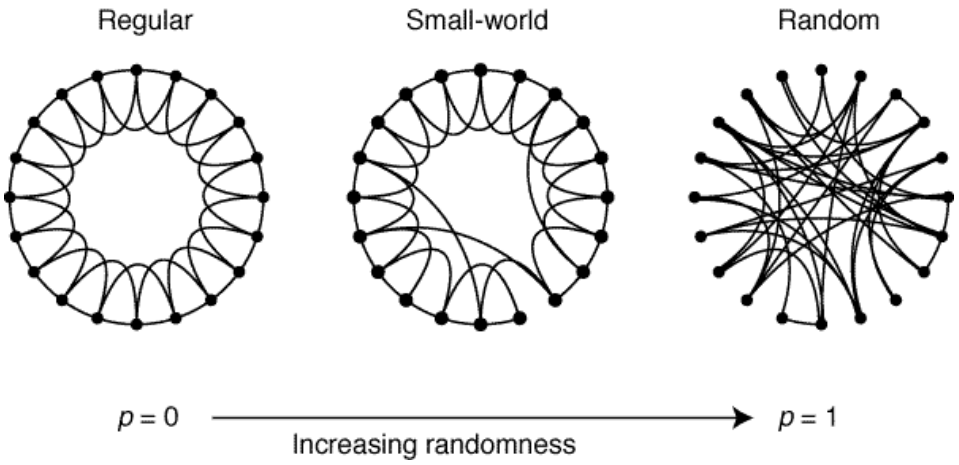

Figure 2.12 – Examples of network architectures. The left graph is a network with 16 vertices where each one binds to four neighbours. This is a regular/ordered graph that has a high ClusC and a long path length. In the case of p = 1 the graph becomes entirely random and has low ClusC and a short path length. Lower p values arise as attributes called “small world”, which combine high ClusC values with short path length.(24)

2.5 State of the art of brain connectivity in Parkinson’s Disease

The DTI technique has become one of the most important tools used for the study of white matter structure in the normal brain,(26,29) while fMRI has become a technology reference for validating the results provided by the DTI method.(5,29,30)

One of the ways to measure water motion is through anisotropy (FA). Lower FA values mean a decrease in fibre coherence of connecting tracts and higher MD values translate to an increase of diffusivity of water molecules in intra- or extracellular spaces.(26,29)

Many studies mention that FA is extremely sensitive, but that it is not a very specific biomarker of neuropathology.(44,45)

However, several investigations have demonstrated that a DTI is certainly a sensitive marker of neuropathology. In this study, MD, FA and connectivity metrics were used as sensitive markers of neuropathology.(44,45)

Numerous studies (structural, functional and effective brain connectivity studies) and clinical applications using DTI have been performed in PD patients.(30–32) Theories have been suggested about the brain structures affected. Normally, the studies are based on the analysis of ROIs, and use voxel-based analysis (VBA) to study the structural changes in PD.(31–34)

Preliminary work has shown that DTI may have an important role in the diagnosis of PD.(21) In fact, in most studies, the FA value in SN on DTI was lower among PD subjects when compared to healthy controls and correlated inversely with the clinical severity of PD.(29) According to Claire J. Cochrane and Klaus P. Ebmeier (29), DTI may be a favourable biomarker in Parkinsonian syndromes. However, they suggest combining the DTI biomarker with another biomarker due to the complexity of these syndromes.(29)

Normally PD is manifested by motor symptoms asymmetrically. Prakash et al.(35) investigated 11 patients with PD and 12 healthy patients, and they observed that MD and FA values are significantly different between the two hemispheres in the rostral SN of patients with PD ($p<0.005$ and $p<0.00005$, respectively).(35) These patients presented with significantly higher MD values in the left rostral SN than healthy patients.(35)

Other studies using DTI have shown the importance of this technique. Anna Hotter demonstrated abnormal results in patients with PD on DWI that have rarely been reported.(35) The same author detected a reduction in FA in the SN and 11 ROIs along a line between the SN and striatum segmented on axial slices of seven patients with early PD.(35) She interpreted this result as a sign of the well-known damage of nigrostriatal projection in early PD.(35) Other authors found reduced FA values in the white matter of the premotor area in advanced PD cases. Scherfler et al.(36) found MR structural modifications of the olfactory region in patients with PD (they applied voxel-wise analysis on trace maps).(36) These results confirmed clinical findings, in other studies, of hyposmia in PD.(36) However, Yoshikawa K et al.(37) investigated possible changes in FA in the nigrostriatal pathway in PD patients. They studied 12 patients with PD and eight Controls using DTI technique.(37) The FA values (ROI defined by the line between the SN and the lower limit of the putamen) were compared with equivalent measurements in Control subjects.(37) They found that there was a significant decrease of these values in patients, even at an early stage of the disease.(37) These results again reinforced the theory that the decline in FA is closely connected with the loss of dopaminergic neurons in subjects with this disease.

In 2013, Baradaran N et al.(30) submitted ten patients with PD and ten Controls to functional MRI tests (fMRI) to determine the pattern of connectivity associated with clinical stiffness found in patients with PD.(30) They also examined the connection between this clinically proven stiffness and motor performance metrics.(30) They

found that cortical and extensive subcortical networks are associated with this rigidity observed in patients with PD, which supports and reinforces the importance of the change in functional connectivity in subjects with PD.(30)

Massimo F et al.(31) analysed the functional connectivity in patients at an early stage of PD, using 69 patients including 44 on medication to affect dopaminergic Control (tPD), and 25 without relevant medication (nPD) and 27 Controls. tPD showed reduced functional connectivity in the striatum and thalamus and augmented functional connectivity in the temporal and occipital regions compared to Controls and nPD.(31) They also found that both tPD and NPD subjects with major motor weakness showed a higher increment in effective connectivity in the thalamus and striatum region.(31)

In addition, graph theoretical analysis has been used in several studies to show brain-behaviour covariance patterns, nodal strength, latent variable values, caudate dopamine transporter (DaT) uptake modularity of the intellectual circuitry and caudate DaT binding in patients with PD.(32) One of the main aims of these studies was to explore the resting state fMRI correlation to cognitive impairment in patients with PD, and to measure the impact of dopamine deficiency on brain systems.(5,8,32) In one of these studies, thirty PD patients with resting state fMRI were included from the PPMI database.(32) The authors also examined 18 patients from this sample with 123I-FP-CIT SPECT. They found that PD-related executive impairment was related to altered stability between cortical and subcortical processing at rest, when the influence of the dorsal cortex became abnormally suppressed, and subcortical processing was disinhibited.(32)

Despite the value of these studies, a multimodal approach and graph theoretical analysis have not yet been applied together for illuminating the brain mechanisms of PD.(32)

The DTI methodology based on graph theory was also used in some studies with PD patients to define and describe the specific connections between different areas in the brain, specifically in different regions of GM, and to estimate also the relationships between them, using a combination of the anatomical connectivity measures obtained and correlations with neurocognitive and motor evaluations.(38) This methodology enables the underlying neural mechanism in the early stages of PD to be described.(38) Batista K et al.(38) used graph theory methodology with DTI to quantify the anatomical connectivity between GM zones through three measures: anatomical connectivity strength (ACS), anatomical connectivity probability (ACP)

and anatomical connectivity density (ACD).(38) They revealed that cognitive and motor deterioration in the early stage of PD is connected with microstructural WM damage extended to the frontal, parietal and temporal regions.(38) They suggested that DTI combined with neurocognitive tests would be a valuable biomarker for identifying cognitive impairment in PD.(38)

Sousa et al.(21) found changes in structural connectivity measures in PD patients. In particular, a decrease in node degree and an increase of MD in the Globus Pallidus, and a decrease of FA in the nucleus accumbens were observed.(21) They also found an increase of brain connectivity in the parahippocampal gyrus (anterior region).(21) Between brain hemispheres, they found changes in the hippocampal, postcentral, precentral, planum temporale and temporal superior (posterior region) gyrus.(21)

Ticló et al.(22) also studied, using a similar methodology, two groups of PD subjects in different disease stages (*de novo* PD and PD 2 to 5 years) and compared them to a Control group over one year.(22) The authors found that FA was consistently augmented in the frontal cortex, suggesting a compensation for the reduction of FA in other areas classically affected by PD.(22) They also detected a decrease in the number of connections of the neural network in PD 2 to 5 years, 1 year after the first acquisition.(22) Finally, a reduction of transitivity, number of edges and network density in PD 2 to 5 years was also observed in comparison to the Control group.(22) Consequently, connectivity analysis may be useful in earlier PD diagnosis biomarker investigation, and for this reason, new studies are suggested with a larger number of patients.(22)

3. Materials and Methods

In this section, the PPMI database will be described, followed by a description of the subject groups and the MRI protocols that were used. At the end of this section, the method of processing and analysis of data implemented by the MIBCA toolbox, as well as the statistical methods used with SPSS, will be explained.

3.1 Parkinson's Progression Markers Initiative database

The PPMI database (https://ida.loni.usc.edu/) was the source of the data used in this thesis.

Our population consisted of 1071 adults, aged 38 to 82 years old, and included patients with normal cognitive state, SWEDD and PD.

The following factors were taken into consideration when selecting the sample: at the time of the examinations, some subjects were taking dopaminergic medication and their T1-w and DTI exams were performed after 12 months of diagnosis. The first group represented the healthy group, the second represented the patients with SWEDD and the last group represented subjects diagnosed with PD. The characterization of those groups (number of patients, gender, age, UPDRS) is shown in Table 3.1.

Table 3.1 – Characterization of Subject Groups – Demographics, Years of Education and UPDRS

	Control	SWEDD	PD
N	30	29	29
Gender	9F/21M	13F/17M	11F/19M
Age*	60.3 ± 9.6* [40–75]	61.8 ± 6.4* [47–80]	59.7 ± 7.6* [44–72]
Years of Education*	16.6 ± 2.6 *	15.5 ± 5.1*	16.8± 1.6*
UPDRS*	2.8 ± 3.0[b] [0–13]	26.3 ± 15.0 [7–64]	32 ± 13.0[a] [13–70]

*Mean ± standard deviation (SD); age range, years of education range and UPDRS range; a) Mann-Whitney test (UPDRS): significant difference between Control and PD (p=0.000); b) significant difference between (UPDRS) Control and SWEDD (p=0.000). No more significant differences were observed.

3.2 Neuroimaging protocols

The MRI protocols used in this research included T1-w and DTI using a 3T MRI scanner (TrioTim, SIEMENS, Erlangen, Germany) and an 8-channel head coil. T1-w sequence (3D MP-RAGE) parameters included sagittal plane acquisition; 240 slices; repetition time (TR)/echo time (TE)/ inversion time (TI)=2300/2.98/900 ms; flip angle=9.0 degrees; matrix=240 x 256; voxel size=1.0 x 1.0 x 1.2 mm^3.

DTI sequence (2D echo-planar imaging) included coronal plane acquisition; 116 slices; TR/TE=890/88 ms; flip angle=90 degrees; 64 gradient directions; b=0, 1000 s/mm^2; matrix=1044 x 1044; voxel size=2 x 2 x 2 mm^3.

3.3 MIBCA Toolbox

The MIBCA Toolbox is an application designed in MATLAB.(39,40) It is an automated all-in-one connectivity analysis toolbox.(39,40) Usable raw data consist of anatomical magnetic resonance imaging (aMRI), diffusion magnetic resonance (dMRI), functional magnetic resonance (fMRI) and positron emission tomography

(PET).(39) The raw data is automatically preprocessed using pipelined software, specifically Freesurfer, Diffusion Toolkit, FSL, SPM and Brain Connectivity Toolbox. MIBCA processes aMRI from T1-w images, dMRI from DTI, fMRI from blood oxygen level dependent on resting state or task-related data and also PET (the last two modalities were not used in this study).(39,40)

The toolbox identifies and processes automatically the different subjects in batches and specifically for each modality following a data folder hierarchy.(39)

In this study only the aMRI and DTI modalities were used. aMRI is the first modality to be processed by the MIBCA toolbox (39,40) and is mandatorily required because it is used to compute the non-linear transformation that is additionally applied to all other modalities.(39) An important step prior to the data preprocessing is the conversion of the images (DICOM) into Nifti format.(39,40) The second step (affine registration, segmentation, intensity normalization) consists firstly in the registration of anatomical images to the Tailarach space using the Freesurfer software,(39,40) followed by brain extraction (results were skull-stripping), correction of intensity inhomogeneities, segmentation into GM, WM and CSF and normalization of WM intensity to 150.(39,40) Other steps are applied such as affine and non-linear registration to the Montreal Neurological Institute (MNI) 305 atlas, and parcellation into cortical and subcortical ROIs according to the Desikan-Killiany-Tourville atlas (all these steps were performed by Freesurfer).(39) In this work, the following were usedas imaging metrics: the cortical thickness (CThk), cortical volume (CVol) and cortical area (CAr) for cortical ROIs.

In dMRI, the images are converted (preprocession data) to Nifti format. In the conversion process b-values and bvec (gradient vector file) files are generated for posterior analysis of the data.(39,40) In the next step, the eddy currents correction is adjusted using eddy_correct (available through FSL), and the DTI estimation is performed using the dti_recon function (available through Diffusion Toolkit).(39) The MD, FA and ADC main eigenvector maps are estimated from cortical and subcortical areas.(39,40) To generate the streamlines from diffusion data, deterministic fibre tracking was used, which is achieved with the Diffusion Toolkit using the FACT algorithm.(39) The generated track is smoothed with the spine_filter of the Diffusion Toolkit and loaded into MATLAB.(21,39) The T1-w image was then affine registered to the b0 diffusion image, and the transformations applied to the atlas image were registered to the T1-w (obtained through the aMRI pipeline).(21,39) Finally, in order

to extract the mean MD, FA and fibre count for each ROI, the registered atlas image is used.(21,39).

After the preprocessed and processed approach, intra-modality and inter-modality group analysis can be performed.

In this study, the MIBCA toolbox calculated automatically for each of the studied groups (Control, SWEDD and PD) the mean and standard deviation for each group.(39) Furthermore, from fibre tracking data, structural connectivity matrices were automatically calculated by determining the number of fibres connecting each ROI pair (FiberConn).(39) The node degree (Deg), clustering coefficient (ClusC), Betweenness centrality (Betw) and Betweenness edge (Edge Betw) metrics were calculated using graph theory.(39,40)

Overall, the matrices and metrics from T1-w data, DTI (imaging metrics) and connectivity metrics were estimated for all 96 regions of interest (ROIs). Table 3.2 summarizes the data processing and analysis implemented in this study.

Table 3.2 – Analysed Modalities and Associated Pre-Processing and Extracted Metrics

Modality	Metrics
T1	Cortical thickness (Cthk), cortical volume (Cvol), cortical area (CAr)
DTI	Mean diffusivity (MD), fractional anisotropy (FA)
Connectivity metrics	Node degree (Deg), clustering coefficient (ClusC), betweenness centrality (Betw), fibre count (FiberConn), betweenness edge (Edge Betw) and distance (Dist)

3.4 Statistical data

Characterization of subject groups regarding age, gender, years of education and Unified Parkinson's Disease Rating Scale (UPDRS) scores was analysed regarding mean, standard deviation, range values and absolute frequency values, when appropriate, using IBM's SPSS. Normality tests were performed to examine whether data had normal distributions, including the Kolmogorov-Smirnov and Shapiro-Wilk tests. Comparison of subjects' demographic data between groups was achieved

using parametric and non-parametric tests (Chi-square, Student T or Mann-Whitney U tests as appropriate).

Directly by using MIBCA, statistical differences were calculated between two groups for each imaging and connectivity metric. A $p < 0.05$ (2-tailed) was chosen as the significance value for all tests.

4. Results and Discussion

In this section, group demographic characterization will first be exposed and discussed. Further, imaging and connectivity results will be presented and analysed.

4.1 Group Characterization

Firstly, the descriptive results were explored involving the variables age, years of education and UPDRS, followed by Shapiro-Wilk and Kolmogorov-Smirnov tests to check the normality of distribution of the variables cited before with a $p < 0.05$ (2-tailed) (Table 4.1).

Age was observed to have a normal distribution since the p-value was higher than the significance used in this research. On the other hand, years of education and UPDRS showed a lower p-value than the significance, so these variables did not have normal distributions.

With regard to the variations in UPDRS scores of each subject by case, significant differences were found between the Control group and the other two groups of study (Figure 4.1). The UPDRS scores were observed to be increased in the PD group compared to the Control.

Table 4.1 – Kolmogorov-Smirnov and Shapiro-Wilk Normality tests

	Case	Kolmogorov-Smirnov			Shapiro-Wilk		
		Statistics	N*	Sig. (p-value)	Statistics	N*	Sig. (p-value)
Age	CONTROL	0.082	30	0.200	0.958	30	0.276
	SWEDD	0.131	29	0.197	0.956	29	0.239
	PD	0.120	29	0.200	0.958	29	0.282
YrsEdu*	CONTROL	0.209	30	0.002	0.952	30	0.195
	SWEDD	0.106	29	0.200	0.941	29	0.095
	PD	0.270	29	0.000	0.860	29	0.001
UPDRS	CONTROL	0.269	30	0.000	0.797	30	0.000
	SWEDD	0.182	29	0.012	0.904	29	0.011
	PD	0.100	29	0.200*	0.953	29	0.207

*N: Number of subjects; Age in years old; YrsEdu = Years of Education; UPDRS = Unified Parkinson's Disease Rating Scale; Sig= Significance.

Figure 4.1 – Box plots displaying significant variations of distribution between the Control (0), SWEDD (1) and PD (2) groups, concerning UPDRS scores of each subject.

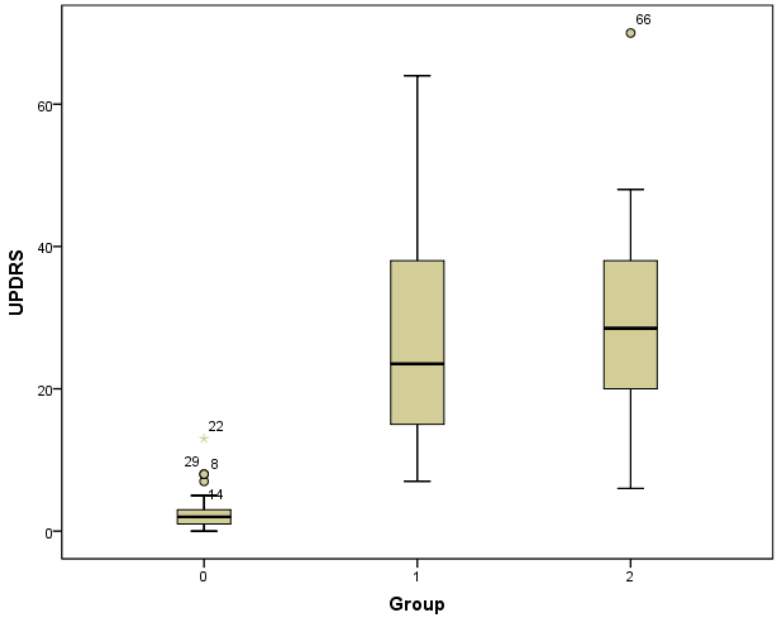

Significant differences were also found (Tables 4.2 and 4.3) regarding the UPDRS data (Mann-Whitney U test) between the Control and PD groups (p = 0.000), and Control and SWEDD groups (p = 0.000) (Table 6). These results are in line with the literature.(21,22) No differences between SWEDD and PD were found. This was to be expected since the differences in clinical findings and neuropsychological tests are very subtle or non-existent, rendering diagnosis of both diseases very difficult.(33,41)

The statistical tests were performed to the three groups: age (Student T-test; p = 0.548), gender (Chi-square test; p = 0.563) and Years of Education (Kruskal-Wallis test, p = 0.472). Those results imply that differences between groups that may be found in subsequent analysis should be related to the pathology or to another variable not considered.

To understand whether differences existed between the groups (variable age) of Control, SWEDD and PD subjects, an ANOVA test was performed and no significant differences were found between the groups (p = 0.635).

Table 4.2 – Mann-Whitney test

Case	UPDRS
Control vs SWEDD	p = 0.000
PD vs CONTROL	p = 0.000

Table 4.3 – Kruskal-Wallis test

Control_SWEDD_PD	UPDRS
CONTROL	p = 0.000
SWEDD	
PD	

4.2 Analysis of Imaging and Connectivity metrics

Normally, the dopaminergic neurons, responsible for neurotransmission, and the damage to major pathways are followed by a reduction of dopamine levels in the caudate nucleus and putamen in PD.(33,41) As mentioned previously, these neurons innervate the basal ganglia, in terms of the dorsal striatum (caudate nucleus

and putamen), central striatum (nucleus accumbens and olfactory tubercule), substantia nigra, globus pallidus, ventral pallidum and subthalamic nucleus. In addition, many studies referred to other structures that are usually damaged, such as the hypothalamus, thalamus, motor cortex, prefrontal cortex (orbitofrontal cortex), oculomotor nuclei and other structures (temporal, parietal, occipital lobes and cerebellum).(33,36,41) The five major pathways in the brain connecting other brain regions with the basal ganglia affected in PD are: motor, oculomotor, associative, limbic and orbitofrontal circuits.(36)

In this section, connectograms were made, analysed and compared to each of the 96 anatomic regions of the brain with the respective imaging and connectivity metrics changes. Finally, the results were compared to previous studies.

As previously stated in the Material and Methods section, the imaging metrics analysed were CThk, CAr, CVol, FA and MD, and lastly, the connectivity metrics were ClusC, Deg, Betw and Edge Betw.

In Table 4.4, the acronyms for each T1-w, DTI, connectivity metric and brain anatomical region used in this work, as well as their designations, are described.

Table 4.4 –The acronyms and designations for all metrics and brain anatomic regions

Acronyms	Designations
CThk	Cortical thickness
CAr	Cortical area
CVol	Cortical volume
FA	Fractional anisotropy
MD	Mean diffusivity
ClustC	Cluster Coefficient
Deg	Node degree
Betweenness centrality	Betw
FiberConn	Number of fibres connecting pair areas
Dist	Distance matrix
Edge Betweenness	Edge Betw
Rh	Right hemisphere
Lh	Left hemisphere
C	Cortex (suffix)
L	Lobule (suffix)
G	Gyrus (suffix)
FP	Frontal pole
ITG	Inferior parietal
MTG	Middle temporal
STG	Superior temporal
TTG	Transverse temporal
SMG	Supra marginal
SPL	Superior parietal
IPL	Inferior parietal
LG	Lingual
FG	Fusiform
TP	Temporal pole
MeOFC	Medial orbitofrontal
rMFG	Rostral middle frontal
SFG	Superior frontal
LOFG	Lateral orbitofrontal
LOG	Lateral occipital
iCG	Isthmus of the cingulate

caCG	Caudal anterior cingulate
raCG	Rostral anterior cingulate
pCG	Posterior cingulate
caMFG	Caudal middle frontal
PHG	Parahippocampal
ParsO	Pars orbitalis
ParsT	Pars triangularis
ParsOp	Pars opercularis
PCal	Pericalcarine
ERC	Entorhinal
Hip	Hippocampus
Acc	Nucleus accumbens
Cd	Caudate
CC	Corpus Callosum
CCp	Corpus Callosum posterior
CCmp	Corpus callossum mid posterior
CCc	Corpus callossum central
CCma	Corpus callossum mid anterior
CCa	Corpus callossum anterior
Pd	Pallidum
Pt	Putamen
Tha	Thalamus
Amy	Amygdala
Ins	Insula
Cn	Cuneus
PCn	Precuneus
PCG	Precentral
PaCG	Paracentral
PoCG	Postcentral
Bankssts	Banks of the superior temporal sulcus
Cerebll	Cerebellum

4.2.1 Connectivity Analysis Control vs PD

In Table 4.5, all significant regional increases and decreases in T1, DTI and connectivity metrics were observed. However, the main significant regions with two, three and four changes are displayed in bold, underlined and in italic, respectively.

The analysis was performed taking into account the number of changes in each hemisphere.

In the first comparison (Table 4.5) between Control and PD (Control vs PD), three metric alterations were observed on the right hemispherical (Rh) pars triangularis (Rh-parsT) regarding an increase in CAr and MD and decrease in FA. This result was confirmed in the literature and perhaps can explain the visuospatial deficits and the emergence of hallucinations in PD patients.(42)(43)

In this research, the right nucleus accumbens (Rh-Acc) showed an increase in FA and Edge Betw, and a decrease in MD. However, this result contradicts the literature. Normally, there is a reduction in FA and an increase in MD.(46,47) This controversial finding can possibly be explained by dopamine medication administration (this medication can change the real values of metrics).(21,22,33) In the left hemisphere (Lh) a decrease of MD and ClusC and an increase of Edge Betw was observed in Cerebll Left (L). These results are in line with previous studies and may be explained by the damage to dopaminergic neurons (the connections with the basal ganglia), and may possibly explain the akinesia/rigidity, tremor gait disturbance, dyskinesia and some motor symptoms characteristic of PD.(48,49) These results confirm the effects of PD outside the basal ganglia affecting other brain regions.

The brain region with the most metric changes (four or more alterations) was the Lh pars orbitalis (parsO) with an increase in Car and MD, and a decrease in FA and Betw. The parsO, also known as Brodmann area 47 (inferior frontal gyrus), is responsible for several functions, such as language (semantic processing, encoding lexical inflection, selective attention to speech and other language functions), memory (working memory and episodic long-term memory) and other functions (behavioural and motor inhibition, adverse emotional inhibition, smelling familiar odours).(50,51) Several studies have demonstrated that apathy resulted from PD. This may be due to the damage of dopaminergic neurons within this brain area.(50,51)

Additionally, decreases in FiberConn (Figure 4.2) in the basal ganglia and corpus striatum regions included: Rh-thalamus (Tha), Putamen (Pd) bilaterally and Rh-Hippocampus (Hip). Lesions on the brain due to PD can affect the dorsal striatum and cause involuntary movements or tremors and also lead to symptoms and signs suggestive of hypothalamic dysfunction.(34,52) Intriguingly, an increase in fibre connections was observed between the Lh-Cuneus (Cn) and the Rh-lateral occipital gyrus (LOG), as well as a decrease between the Lh-rostral middle frontal (rMFG) and the Rh-frontal pole (FP). These results can possibly be explained by a compensatory effect in compensating for the weakness in movement control typically resulting from this pathology.(34)

With regard to the Dist and Edge Betw in Figure 4.2, the differences observed were major in the occipital and temporal regions and more minor in Rh-Ins and Rh-ITG, respectively. Once again, the occipital and temporal regions can possibly compensate for the depression of dopamine levels in neurons.(34) As regards the Rh-Ins and Lh-ITG, the reduction of Edge Betw may once again be due to damage to dopaminergic neurons and may disturb the limbic region (ITG) and the capacity for perception and motor control (usually in PD).(53)

Table 4.5 – Statistical values of all metrics obtained with MIBCA software for comparison between Control and PD, regarding the T1, DTI and connectivity metrics. Significant values are considered for $p < 0.05$. Δ is the statistical difference. Red and Blue squares, respectively, represent lower and higher values for the second group in comparison to the first. White squares correspond to non-significant differences.

	CThk (mm)	Car (mm^2)	Cvol (mm^3)	FA	MD	ClustC	Deg	Betw
FP				**Lh**: Δ = 2.92; p = 0.003 **Rh**: Δ = 2.92; p = 0.02	**Rh**: Δ = -2.71; p = 0.007			
SMG								**Rh**: Δ = -1.97; p = 0.049
LG							**Rh**: Δ = 2.05; p = 0.041	
FG	**Rh**: Δ = -1.99; p = 0.046	**Lh**: Δ = -2.14; p = 0.032						
TP		**Lh**: Δ = -2.63; p = 0.008						
rMFG				**Rh**: Δ = 3.05; p = 0.002	**Lh**: Δ = -3.10; p = 0.002 **Rh**: Δ = -2.37; p = 0.018			
SFG		**Lh**: Δ = -1.98; p = 0.048 **Rh**: Δ = -1.24; p = 0.019						
caCG	**Rh**: Δ = -2.36; p = 0.018			**Rh**: Δ = 2.31; p = 0.020				
pCG			**Rh**: Δ = -2.04; p = 0.042					
caMFG				**Lh**: Δ = 2.52; p = 0.011				
PHG	**Rh**: Δ = -1.99; p = 0.046		**Lh**: Δ = -2.30; p = 0.022				**Rh**: Δ = 2.34; p = 0.019	
ParsO		**Lh**: Δ = -2.40; p = 0.016		**Lh**: Δ = 2.31; p = 0.020 **Rh**: Δ = 2.31; p = 0.005	**Lh**: Δ = -1.99; p = 0.046			**Lh**: Δ = 2.03; p = 0.042
ParsT		**Rh**: Δ= -2.14; p =0.032		**Lh**: Δ = 2.77; p = 0.005 **Rh**: Δ = 3.80; p = 1.00e-04	**Lh**: Δ = -2.58; p = 0.009 **Rh**: Δ = -2.36; p = 0.02			
ParsOp				**Lh**: Δ= 2.19; p =0.028				
ERC	**Lh**: Δ = -1.96; p = 0.049	**Rh**: Δ = -2.16; p = 0.031		**Rh**: Δ = 2.22; p = 0.026				
Acc				**Rh**: Δ = -2.16; p = 0.031	**Rh**: Δ = 2.28; p = 0.022			
CCp				Δ = -3.22; p = 0.001				

	CThk (mm)	Car (mm^2)	Cvol (mm^3)	FA	MD	ClustC	Deg	Betw
CCmp					Δ = 2.52; p = 0.011			
CCc					Δ = 2.68; p = 0.007			
Pd					**L**: Δ = 2.78; p = 0.005			
Ins		**Lh**: Δ = -2.02; p = 0.043	**Rh**: Δ = -2.04; p = 0.041					
Cn		**Rh**: Δ = -2.58; p = 0.009						
PCn		**Rh**: Δ = -2.02; p = 0.043						
PCG							**Rh**: Δ = -2.48; p = 0.013	
CerebLL					**L**: Δ = 1.96; p = 0.04 **R**: Δ = 2.33; p = 0.019	**L**: Δ = 2.07; p = 0.038		**L**: Δ = -2.27; p = 0.023

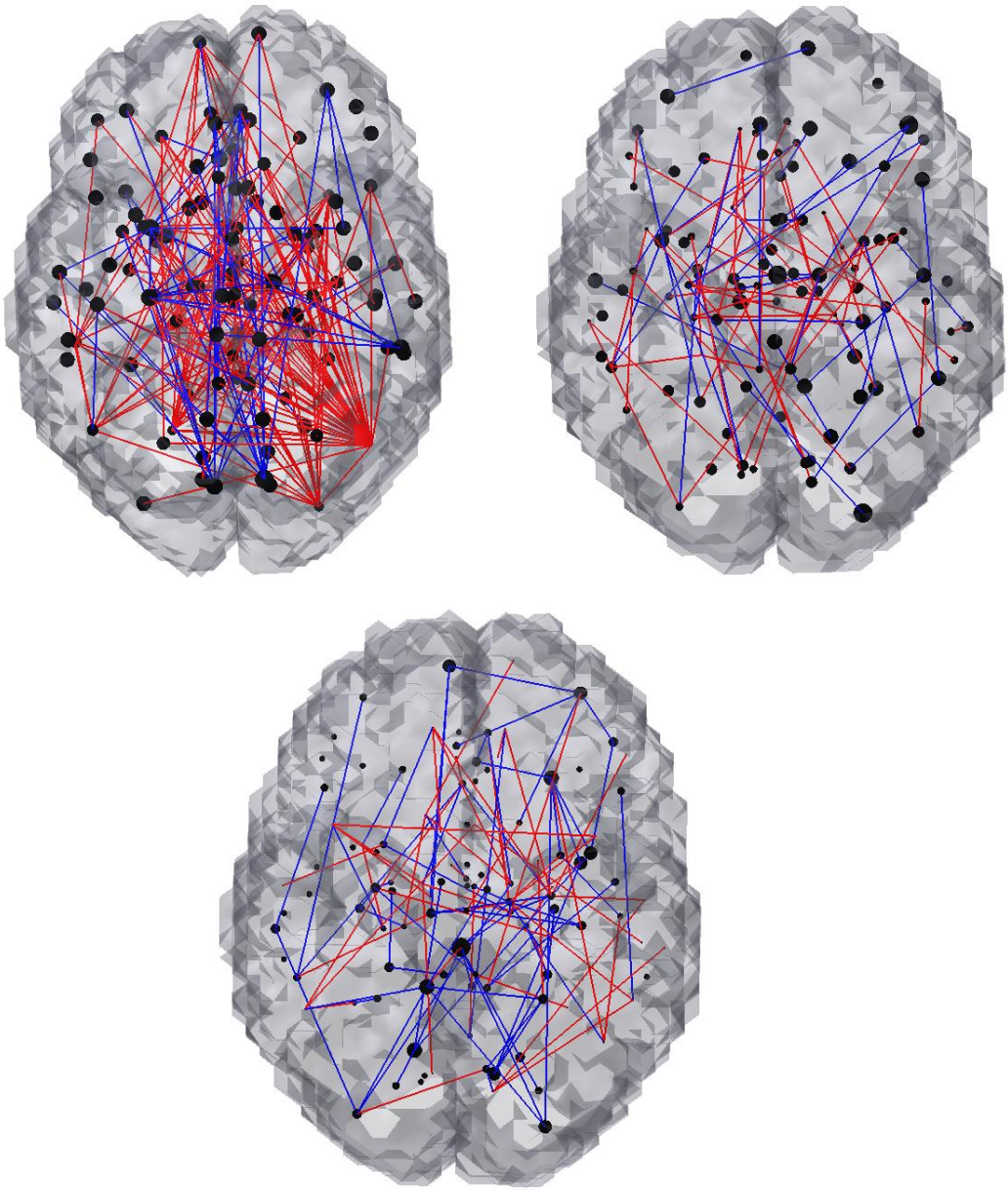

Figure 4.2 – 3D graphs of distance matrix (superior left side), Edge Betweenness (superior right side) and FiberConn (below) of Control vs PD test. Significant values are considered when they were $p < 0.05$. Red and Blue lines, respectively, represent lower and higher values for the second group in comparison to the first.

4.2.2 Connectivity Control vs SWEDD

While there have been many studies using the DWI and DTI techniques in the diagnosis of PD, they have almost entirely made a comparison between healthy individuals and PD patients. As regards SWEDD studies based on brain connectivity and graph theory, they have not, to the best of our knowledge, been published yet.

The main significant alteration was in the insula of both hemispheres with two metric changes, regarding a decrease in MD and increase in ClusC. However, in the Rh-Ins an increase in CVol was observed, whilst in the Lh-Ins an increase of FA was observed instead. This shows that SWEDD differences probably do not have a symmetric manifestation pattern, and curiously, the distance connections in both hemispheres decrease. This last result may be due to the damage to dopaminergic neurons between the basal ganglia and insular cortex. These metric changes may explain, again, the loss of perception and motor control associated with the SWEDD condition.(34,53)

Once again, this test demonstrated that the Cerebll showed connectivity metric changes, regarding this time a decrease in Deg. This reinforces again the theory previously mentioned regarding the damage to dopaminergic neurons in the connections between the basal ganglia and cerebellum.(48,49)

The FiberConn (Figure 4.3) showed a general increase between the subcortical and Rh cortical structures, however the R-Acc, R-Pd and Lh-Tha showed a decreasing number of tracts. Interestingly, the Rh-Tha has a different result, presenting an increase in the number of connections. This contradictory result can be explained by the asymmetrical manifestation patterns of SWEDD.

With regard to Edge Betw (Figure 4.3), the differences observed were generally decreased in all tests, however the parsT showed a marked decrease of its influence in this network (decrease in ClusC). As for Dist (Figure 4.3), in this comparison a generalized increase was observed, especially in the Rh-parsT, which showed a marked increase in its connections with temporal, occipital and basal ganglia regions.

Table 4.6 – Statistical values of all metrics obtained with MIBCA software for comparison between Control and SWEDD, regarding the T1, DTI and connectivity metrics. Significant values are considered for $p < 0.05$. Δ is the statistical difference. Red and Blue squares, respectively, represent lower and higher values for the second group in comparison to the first. White squares correspond to non-significant differences.

	CThk (mm)	Car (mm²)	Cvol (mm³)	FA	MD	ClustC	Deg	Betw
FP	**Rh:** Δ = 2.10; p = 0.036		**Rh:** Δ = 2.60; p = 0.009					
ITG					**Lh:** Δ = 2.07; p = 0.038			
SMG				**Lh:** Δ = -2.62 p = 0.009 **Rh:** Δ = -2.10 p = 0.036	**Lh:** Δ = 2.19; p = 0.028 **Rh:** Δ = 2.01; p = 0.044			
SPL		**Lh:** Δ = -2.34; p = 0.019		**Lh:** Δ = -1.99; p = 0.046 **Rh:** Δ = -1.99; p = 0.048				
LG					**Rh:** Δ = 2.39; p = 0.017			**Rh:** Δ = -2.07; p = 0.038
MeOFC					**Rh:** Δ = 2.19; p = 0.029			
rMFG							**Lh:** Δ = -2.28; p = 0.022	
SFG						**Lh**: Δ = -2.42; p =0.016		
iCG				**Lh:** Δ = -2.60; p = 0.009 **Rh:** Δ = -2.33; p = 0.020	**Lh:** Δ = 3.01; p = 0.048			
raCG							**Lh:** Δ = -1.99; p = 0.047	
ParsO	**Lh:** Δ = 2.10; p = 0.036	**Lh:** Δ = -2.30; p = 0.022			**Rh:** Δ = 1.06; p = 0.049			
CCp					Δ = 1.99; p = 0.049			
Pd					**L:** Δ = 1.51; p =0.041 **R:** Δ = 2.39;;; p =0.017			
Ins			**Rh:** Δ = -2.34; p = 0.019	**Lh:** Δ = -1.98; p = 0.048	**Lh:** Δ = 2.27; p =0.023 **Rh:** Δ = 2.62; p = 0.009	**Lh:** Δ = -2.08; p = 0.037 **Rh:** Δ = -2.28; p = 0.012		
PCn						**Rh:** Δ = -2.24; p = 0.025		

	CThk (mm)	Car (mm^2)	Cvol (mm^3)	FA	MD	ClustC	Deg	Betw
PaCG				**Lh:** Δ = 2.86; p = 0.004				
PoCG				**Lh:** Δ = -3.20; p =0.018 **Rh**: Δ = -2.37; p = 0.001				**Rh:** Δ = -2.06; p = 0.039
Bankssts				**Lh:** Δ = -2.51; p = 0.001	**Lh:** Δ = 2.13; p = 0.033			
CerebII					**R:** Δ = 1.96; p = 0.049		**R:** Δ = 2.21; p = 0.027	

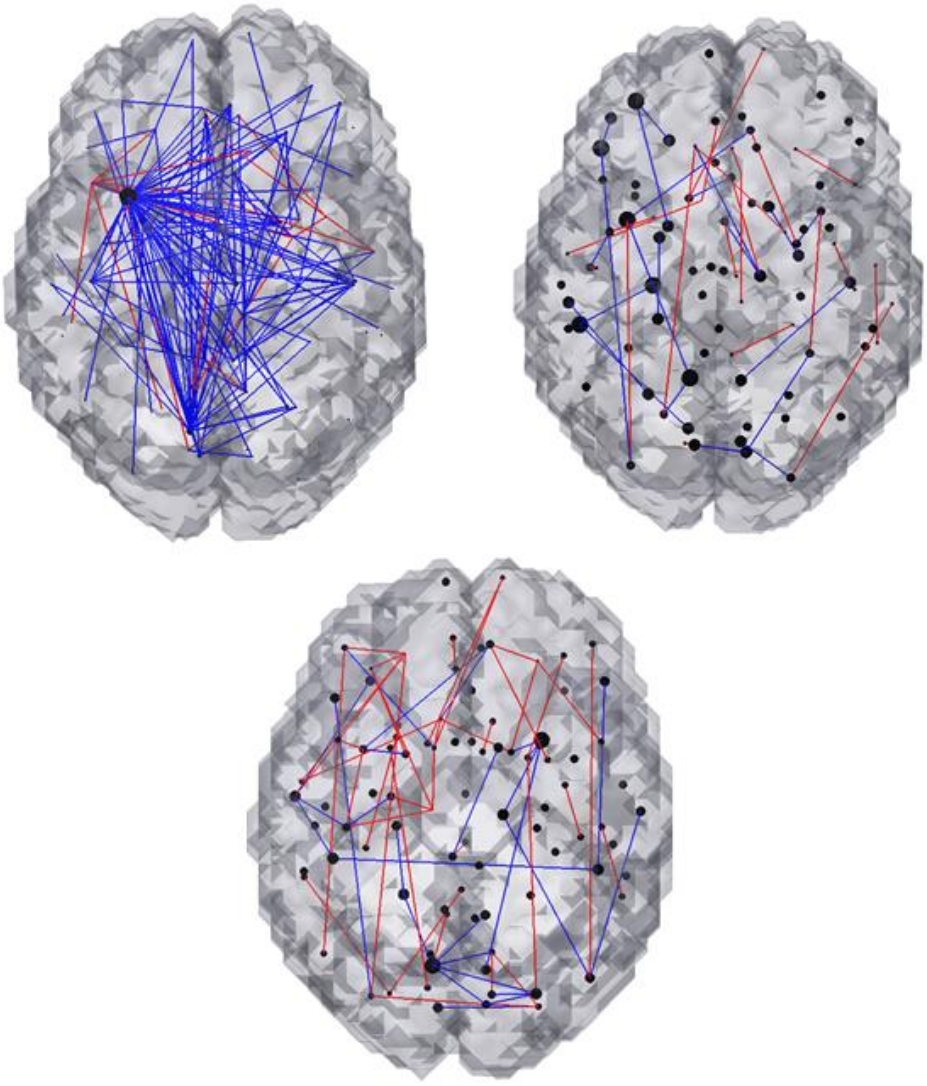

Figure 4.3 – 3D graphs of distance matrix (superior left side), Edge Betweenness (superior right side) and FiberConn (below) of Control vs SWEDD test. Significant values are considered when they were $p < 0.05$. Red and Blue lines, respectively, represent lower and higher values for the second group in comparison to the first.

4.2.3 Connectivity SWEDD vs PD

The last two groups compared were SWEDD and PD (SWEDD vs PD). In this comparison (Table 4.7) the differences between these groups were observed to be more extensive than in the other comparisons. In particular, additional changes were observed in the temporal lobe regions and frontal lobe regions, regarding Brodmann 44, 45 and 47 areas bilaterally (pars opercularis, pars triangularis and orbitalis).(34,53) It is also important to mention that Brodmann 44 and 45 include Broca area (the major function of this area is language processing).(48,53) PD normally affects this area and causes speech difficulties, such as a soft, monotone voice, slowed hesitant speech or rapid stuttering speech.(50,51)

The Ins (Brodmann area 33) in both hemispheres presented connectivity changes in terms of a decrease in FA and increase in MD.

Further, the parahippocampal gyrus (PHG) bilaterally showed significant changes, concerning CVol, an increase in MD and decrease in FA. A lack of dopamine (stimulation) or denervation of PHG can cause atrophy of this region and furthermore memory impairment.(50,53) Additionally, these judgements can show the predisposition of the salience network in PD and its potential role in memory and executive dysfunction.(53)

Another region with significant metric alterations was Rh-rMFG, with an increase in cortical thickness (CThk) and CVol, and a decrease in FA (in both hemispheres). The alterations in this region were mentioned before along with the nigrostriatal dopaminergic damage.(51,53)

Moreover, the Rh banks of the superior temporal sulcus (bankssts) demonstrated an increase in MD and decrease in FA (bilaterally) and Betw. The bankssts presents multisensory processing capabilities, and with these findings, the lack of dopamine in this region can likely result in the deterioration of visuoperceptive integration.(54)

The FP was the region that presented most connectivity changes in this comparison, in terms of an increase in CThk and CVol and a decrease in FA (in both hemispheres) and Deg. The presence of this finding in this lobe may have several explanations. As mentioned previously, decreases of FA values in the frontal lobe and other structures are in line with the literature (the changes may occur outside the SN and in the rest of the basal ganglia),(34,53) resulting from the damage to dopaminergic neurons. Second, diffusion changes may be reflective of frontal lobe dysfunction in PD.(42) Many fMRI studies have shown alterations in activation in

motor and premotor areas in PD during the performance of motor tasks, particularly in the supplementary motor area.(34,53) Dysfunction of the frontal lobe, which probably derives from alterations in basal ganglia connections due to nigrostriatal dopaminergic damage, plays a role in impaired motor performance resulting in hypokinesia.(53) This finding is supported by brain imaging studies (such as conventional MRI, fMRI and PET) showing reduced local blood flow in the supplementary motor area and the prefrontal region.(9,50) Morphologic longitudinal imaging studies have revealed significant brain volume loss in patients with PD without dementia compared with healthy patients.(50,51) Frontal lobe alterations were found in patients with PD with early cognitive impairment and those with or without dementia. However, frontal lobe atrophy, which can occur with the duration of the disease, has been described in the late stage of PD. The results of this study complement these other studies in demonstrating that diffusion metric changes can occur in the frontal lobe in patients with PD (52,53). (However, atrophy was not found in the FP in this comparison and in Control-PD, except in Control-SWEDD comparison.)

Once again, Lh-Cerebll presented connectivity metric changes, such as an increase in Deg and decrease in ClusC.

Interestingly, both hemispheres showed marked decrease in the number of fibre connections (Figure 4.4), especially Rh-Hip. With regard to the Dist, a high and marked decrease was observed (Figure 4.4) for intra- and interhemispheric areas in the whole brain. Reductions of intrahemispheric and augmentation of interhemispheric Edge Betw were also observed (Figure 4.4). Both findings can perhaps show the state of deterioration of PD compared to SWEDD, demonstrating the potential of this methodology for differentiating between these two neuropathologies.

Table 2.7 – Statistical values of all metrics obtained with MIBCA software for comparison between SWEDD and PD, regarding the T1, DTI and connectivity metrics. Significant values are considered for $p < 0.05$. Δ is the statistical difference. Red and Blue squares, respectively, represent lower and higher values for the second group in comparison to the first. White squares correspond to non-significant differences.

	CThk (mm)	Car (mm^2)	Cvol (mm^3)	FA	MD	ClustC	Deg	Betw
FP	**Lh:** Δ = -2.13; p = 0.032 **Rh:** Δ = -2.99; p = 0.003		**Lh**: Δ = -2.29; p = 0.022 **Rh**: Δ = -3.40; p = 6.78e-04				**Lh**: Δ = 2.18; p = 0.030	
ITG			**Lh**: Δ = -2.45; p = 0.014 **Rh**: Δ = -2.01; p = 0.044	**Rh**: Δ = 2.25; p = 0.024				
MTG		**Rh**: Δ = -2.32; p = 0.020						
STG				**Lh**: Δ = 2.27; p = 0.023				
TTG				**Lh**: Δ = 2.02; p = 0.043			**Lh**: Δ = 1.99; p = 0.047	
SMG				**Lh**: Δ = 2.64; p = 0.008 **Rh**: Δ = 2.16; p = 0.031				
SPL				**Rh**: Δ =2.86; p =0.004		**Lh**: Δ = -2.71; p = 0.007	**Lh**: Δ = 2.53; p = 0.011	
IPL								**Lh**: Δ = 2.68; p = 0.007
LG							**Rh**: Δ = 2.17; p = 0.030	
FG		**Lh**: Δ = -2.14; p = 0.032						
MeOFC					**Rh**: Δ = -2.47; p = 0.013			
rMFG	**Rh**: Δ =-2.03; p = 0.042		**Rh**: Δ = -2.12; p = 0.034	**Lh**: Δ = 3.47; p = 5.24e-04 **Rh**: Δ = 2.61; p = 0.009			**Lh**: Δ = 3.04; p = 0.002	
SFG			**Lh**: Δ = -2.00; p =0.046 **Rh**: Δ = -2.46; p = 0.014	**Lh**: Δ = 2.86; p = 0.004				
LOFG				**Rh**: Δ = 2.85; p = 0.004	**Rh**: Δ = -2.04; p = 0.042		**Lh**: Δ = 3.32; p = 9.06e-04 **Rh**: Δ = 2.11; p = 0.035	

	CThk (mm)	Car (mm^2)	Cvol (mm^3)	FA	MD	ClustC	Deg	Betw
LOG							**Rh**: Δ = 2.01; p = 0.044	
iCG		**Rh**: Δ = -2.25; p = 0.025		**Lh**: Δ = 2.16; p = 0.031	**Rh**: Δ = -2.10; p = 0.036			
pCG						**Rh**: Δ = 2.11; p = 0.034		
PHG			**Lh**: Δ = -2.15; p = 0.031 **Rh**: Δ = -2.25; p = 0.025	**Lh**: Δ = 2.61; p = 0.009 **Rh**: Δ = 3.34; p = 8.27e-05	**Lh**: Δ = -2.21; p = 0.027 **Rh**: Δ = -2.78; p = 0.005			
ParsO				**Lh**: Δ = 3.23; p = 0.001 **Rh**: Δ = 3.98; p = 6.86e-05	**Lh**: Δ = -2.67; p = 0.008 **Rh**: Δ = -2.64; p = 0.008		**Lh**: Δ = 2.16; p = 0.031	**Lh**: Δ = 2.77; p = 0.006
ParsT				**Lh**: Δ = 2.46; p = 0.014 **Rh**: Δ = 3.42; p = 6.23e-04	**Lh**: Δ = -2.30; p = 0.021			
ParsOp				**Lh**: Δ = 2.32; p = 0.021 **Rh**: Δ = 2.49; p = 0.013				
ERC				**Rh**: Δ = 2.95; p = 0.003	**Rh**: Δ = -2.57; p = 0.010			
CCp							Δ = 2.16; p = 0.031	
Ins				**Lh**: Δ = 3.02; p =0.003 **Rh**: Δ = 2.78; p = 0.005	**Lh**: Δ = -2.11; p = 0.034 **Rh**: Δ = -2.39; p = 0.017			
Cn		**Rh**: Δ = -2.15; p = 0.025		**Rh**: Δ = 2.02; p = 0.043				
PCn		**Rh**: Δ = -2.15; p = 0.031						
PCG				**Lh**: Δ = 2.66; p = 0.008 **Rh**: Δ = 2.07; p = 0.049				
PoCG				**Lh**: Δ = 2.39; p = 0.017 **Rh**: Δ = 2.97; p = 0.003				
Bankssts				**Lh**: Δ = 2.66; p = 0.008 **Rh**: Δ = 2.88; p = 0.004				**Rh**: Δ = 2.16; p =0.031
CerebII						**L**: Δ = 2.46; p =0.014	**L**: Δ = -2.04; p =0.041	

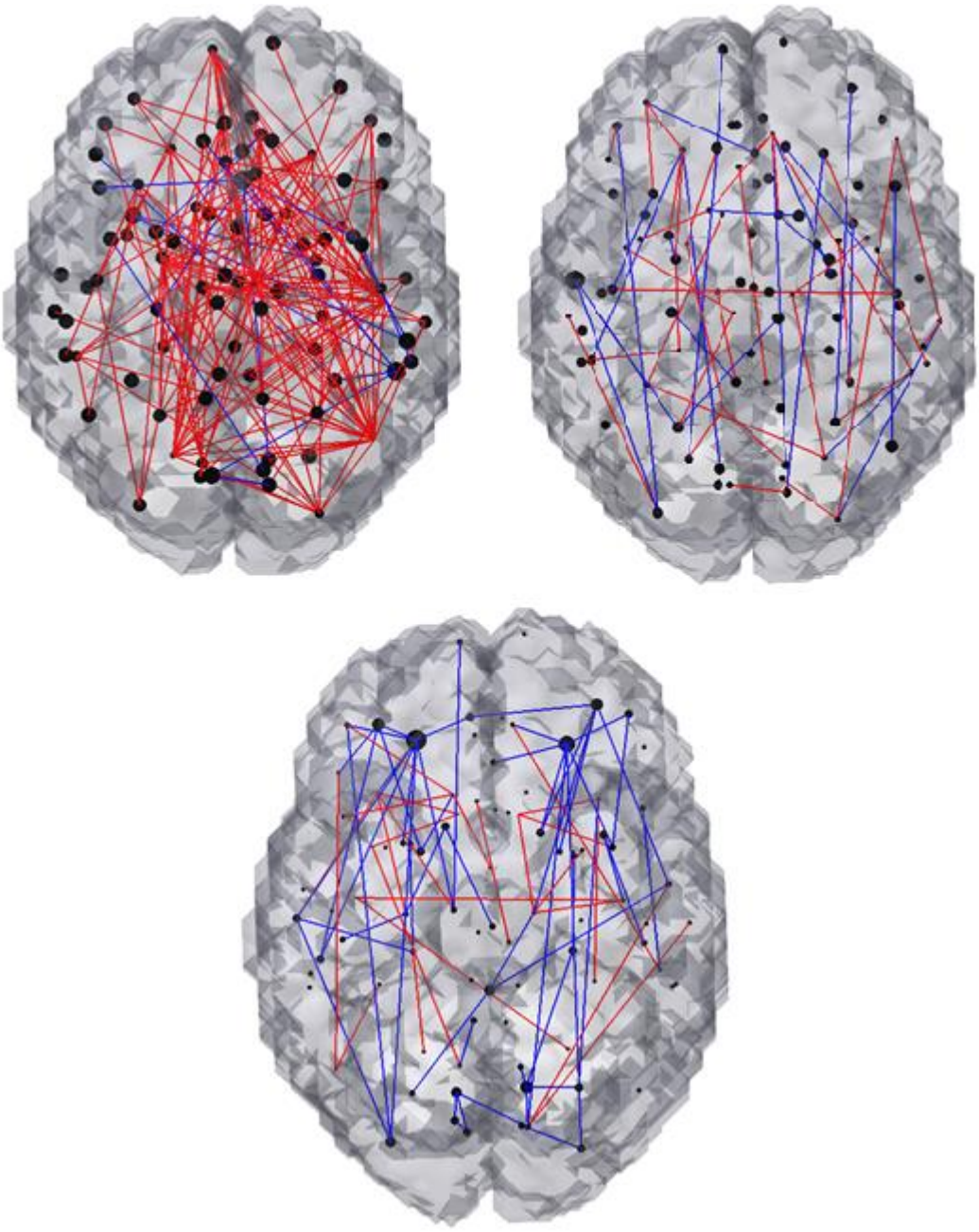

Figure 4.4 – 3D graphs of distance matrix (superior left side), Edge Betweenness (superior right side) and FiberConn (below) of SWEDD vs PD test. Significant values are considered when they were $p < 0.05$. Red and Blue lines, respectively, represent lower and higher values for the second group in comparison to the first.

4.2.4 Overall Connectivity changes

The obtained results are in line with the literature (21,22,24,32) and also contribute to novel knowledge, which should be explored in future studies regarding SWEDD and PD differences. All comparisons performed in this research demonstrated several and sometimes highly marked changes in all kinds of metrics.

The biggest changes were observed in Control vs PD and SWEDD vs PD, whereas between Control and SWEDD changes also existed, but were not so manifest. In Control vs PD patients changes were observed in several metrics, such as a general and marked increase of the CAr mostly in frontal, temporal regions. This comparison demonstrated as well a substantial decrease of the FA and increase of the MD in the whole brain, especially in frontal, temporal and parietal regions. With regard to other metrics, such as FiberConn, Dist and Edge Betw, this comparison revealed numerous decreases in frontal and temporal regions.

As for the SWEDD vs PD comparison, several changes were seen in all metrics, however the most significant change occurred in connectivity metrics, such as in FA, MD, Deg and Dist. Several obvious FA decreases and MD increases were reported, affecting the whole brain. Otherwise, decreases of Deg in frontal, temporal and occipital regions were noticed as well; decreases of fibre connectivity and Edge Betw, especially in basal ganglia and temporal regions, were also noted; and finally, a marked decrease of the Dist in frontal and temporal regions was observed.

5. Limitations and future perspectives

This study, just like other researches, is not without limitations. Firstly, the possible confounding effects of dopaminergic treatments are not considered in our work. To be prudent, future studies are encouraged to take into account the effects of this medication on brain connections. Additionally, probabilistic algorithms were not used. These algorithms have advantages compared to the deterministic methods, given the error associated with each preferential direction of diffusion. Thirdly, the size of the sample was a clear limitation of this study. It would be desirable to carry out a study with a larger number of individuals to confirm the results obtained in this kind of study.

The automatisms of MIBCA (BCT and FSL) software used to calculate the matrices and possible errors in the alignment of images caused by the geometric distortions observed in diffusion images, related to the heterogeneities of the external magnetic field B0 present during the acquisition of the MRI, can be mentioned as one of the possible causes of discrepancies in some of the least expected results, such as the nucleus accumbens showing decreased MD, and increased FA, FiberConn and Edge Betw, which are not to be expected at all, according to the literature. However, in this thesis the same methodology was always used in the calculation of connectivity metrics, making this a positive perspective. In future studies this is a factor to consider and improve, with the intention of reducing the effect of the apparent geometric distortions in diffusion-weighted imaging due to magnetic susceptibility differences. It is suggested that in order to alleviate this problem, the images can be acquired with different phase encodings and an improvement in the correction of geometric distortions.

Regarding the p-value used as reference for the statistical tests (fixed at 0.05) was not Bonferroni corrected. As justification, it was considered that this correction is extremely conservative and it was impossible to exclude the dependence of variables, which could result in a large number of false negatives as well.

It is essential to refer as well to the threshold value used to produce matrices of adjacency, which have a great influence on the values of connectivity metrics. This choice turns out to be greatly influenced by the investigator who leads the investigation, based on educated guesses on setting the threshold, although there are some publications on the use of graph theory in which the threshold value is

adjusted to the group in question. In this study the same threshold level of a significance level of 5% was always used.

Future studies can be considered using other score values in addition to the UPDRS, such as the Mini-Mental State Examination to search for possible cognitive problems, and the Hamilton Rating Scale of Depression to understand and evaluate depression in patients. Another interesting area is fMRI, allied with genetics data, to investigate whether correlations exist and to compare any differences between SWEDD and PD patients.

6. Conclusion

Throughout the literature, most scientific studies performed until now were focused on functional studies in patients with PD, whereas in this study the focus was on structural brain connectivity analysis.

This study was based on analysis of imaging (cortical and diffusion metrics) and connectivity metrics in order to search for structural brain connectivity changes. To achieve this purpose, specific software was used and methods were allied with careful methodology, in terms of the MIBCA software associated with graph theory.

Brain structural connectivity analysis with application of graph theory can be a very powerful method in research, especially in investigating novel biomarkers of disease. This technique enables the acquisition of many connectivity metrics that may indicate morphological and functional changes in each region. The main motivation for using graph theory as a method of analysis in this work was the relative ease of understanding, and the higher degree of generalization and interpretation.

In the first instance, demographic data such as gender, age, years of education and UPDRS scores were compared between groups using parametric or non-parametric tests, as appropriate. Differences between groups were also evaluated regarding imaging and connectivity metrics, and FiberConn, using MIBCA's statistical functions, and differences were visualized in connectograms and brain graphs. Significant differences were found concerning the UPDRS scores between the Control and PD groups, and Control and SWEDD groups.

Furthermore, the application of MIBCA resulted in imaging metrics such as CThk, CAr and CVol obtained from T1-w data for all 96 ROIs, as well as mean diffusibility (MD), fractional anisotropy (FA) and FiberConn from DTI data. Also, SC matrices were computed from FiberConn data, as well as derived connectivity metrics such as Deg, ClusC, Betw, Edge Betw and distance.

In the comparison of Control vs PD, several significant differences were observed regarding various imaging and connectivity metrics, particularly in the basal ganglia of both hemispheres. In the right hemisphere, the nucleus accumbens showed decreased MD and increased FA, FiberConn and Edge Betw. These changes were similarly observed for the rostral middle frontal gyrus (rMFG) of both hemispheres. Finally, changes were also observed for the connection of basal ganglia structures such as the putamen and thalamus. These findings may be related to known

degeneration of dopaminergic pathways, including the mesolimbic, mesocortical and nigrostriatal pathways in PD.

Secondly, in the Control vs SWEDD test, the splenium of the corpus callosum showed decreased MD and Deg and increased FA and FiberConn. Regions of the frontal and parietal lobes showed various connectivity metric changes, particularly the superior marginal gyrus and superior parietal gyrus of both hemispheres and the pars orbitalis of the left hemisphere. These results show changes in different regions to those observed for PD, supporting the idea that SWEDD is a distinct nosological entity, or entities.

In the last comparison, PD vs SWEDD, various DTI-based imaging and connectivity metric changes were observed in the frontal lobe of both hemispheres, particularly in the frontal pole, rMFG and superior frontal gyrus, regions of the mesocortical pathway. In the limbic lobe, changes were observed in the isthmus of the cingulate gyrus and the parahippocampal gyrus of both hemispheres, which may be related to memory impairment. In the insular cortex of both hemispheres a decreased FA and increased MD and ClusC were observed. These findings could be related to cognitive decline, behavioural abnormalities and somatosensory disturbances.

All results observed in this study are in line with the literature (except Rh-Acc findings) regarding observed changes in regions related to the nigrostriatal, mesocortical and mesolimbic pathways.

These findings may suggest that the study of structural connectivity is an important method for distinguishing PD from SWEDD.

Finally, it should be noted that the object of this study resulted in the submission and acceptance of an e-poster, which will be presented in May 2016 at the 24th annual meeting of the ISMRM (International Society for Magnetic Resonance in Medicine) in Singapore, with the name “Scans Without Evidence for Dopaminergic Deficit Patients”.

References

1. Albert R, Barabási A-L. Statistical mechanics of complex networks. Rev Mod Phys. 2002;74(1):47–97. Available from: http://link.aps.org/doi/10.1103/RevModPhys.74.47

2. Bullmore E, Sporns O. Complex brain networks: graph theoretical analysis of structural and functional systems. Nat Rev Neurosci. Nature Publishing Group; 2009 Mar 4;10(4):312–312. Available from: http://dx.doi.org/10.1038/nrn2618

3. Bressler SL, Menon V. Large-scale brain networks in cognition: emerging methods and principles. Trends Cogn Sci. Elsevier; 2010 Jun 6;14(6):277–90. Available from: http://www.cell.com/article/S1364661310000896/fulltext

4. Gong G, He Y, Concha L, Lebel C, Gross DW, Evans AC, et al. Mapping anatomical connectivity patterns of human cerebral cortex using in vivo diffusion tensor imaging tractography. Cereb Cortex. 2009 Mar 1;19(3):524–36. Available from: http://cercor.oxfordjournals.org/content/19/3/524.abstract

5. Lehéricy S, Sharman MA, Dos Santos CL, Paquin R, Gallea C. Magnetic resonance imaging of the substantia nigra in Parkinson's disease. Mov Disord. 2012 Jun;27(7):822–30. Available from: http://www.ncbi.nlm.nih.gov/pubmed/22649063

6. Péran P, Cherubini A, Assogna F, Piras F, Quattrocchi C, Peppe A, et al. Magnetic resonance imaging markers of Parkinson's disease nigrostriatal signature. Brain. 2010 Nov;133(11):3423–33. Available from: http://www.ncbi.nlm.nih.gov/pubmed/20736190

7. Planetta PJ, Schulze ET, Geary EK, Corcos DM, Goldman JG, Little DM, et al. Thalamic projection fiber integrity in de novo Parkinson disease. AJNR Am J Neuroradiol. 2013 Jan;34(1):74–9. Available from: http://www.pubmedcentral.nih.gov/articlerender.fcgi?artid=3669594&tool=pmcentrez&rendertype=abstract

8. Menke RA, Scholz J, Miller KL, Deoni S, Jbabdi S, Matthews PM, et al. MRI characteristics of the substantia nigra in Parkinson's disease: a combined quantitative T1 and DTI study. Neuroimage. 2009 Aug 15;47(2):435–41. Available from: http://www.ncbi.nlm.nih.gov/pubmed/19447183

9. Lee E-Y, Sen S, Eslinger PJ, Wagner D, Shaffer ML, Kong L, et al. Early cortical gray matter loss and cognitive correlates in non-demented Parkinson's patients. Parkinsonism Relat Disord. 2013 Dec;19(12):1088–93. Available from: http://www.pubmedcentral.nih.gov/articlerender.fcgi?artid=3858507&tool=pmcentrez&rendertype=abstract

10. Martin J. Neuroanatomy Text and Atlas. 4th ed. Weitz M, Christie N, editors. New York: Hill, Mc Graw; 2012.

11. Stoessl AJ. Scans without evidence of dopamine deficiency: the triumph of careful clinical assessment. Mov Disord. 2010 Apr 15;25(5):529–30. Available from: http://www.ncbi.nlm.nih.gov/pubmed/20425792

12. Erro R, Schneider SA, Stamelou M, Quinn NP, Bhatia KP. What do patients with scans without evidence of dopaminergic deficit (SWEDD) have? New evidence and continuing controversies. J Neurol Neurosurg Psychiatry. 2015 May 19;87(3):319–23. Available from: http://www.ncbi.nlm.nih.gov/pubmed/25991401

13. Schwingenschuh P, Ruge D, Edwards MJ, Terranova C, Katschnig P, Carrillo F, et al. Distinguishing SWEDDs patients with asymmetric resting tremor from Parkinson's disease: a clinical and electrophysiological study. Mov Disord. 2010 Apr 15;25(5):560–9. Available from: http://www.pubmedcentral.nih.gov/articlerender.fcgi?artid=2996567&tool=pmcentrez&rendertype=abstract

14. Utiumi MAT, Felício AC, Borges CR, Braatz VL, Rezende SAS, Munhoz RP, et al. Dopamine transporter imaging in clinically unclear cases of parkinsonism and the importance of Scans Without Evidence of Dopaminergic Deficit (SWEDDs). Arq Neuropsiquiatr. Associação Arquivos de Neuro-Psiquiatria; 2012 Sep;70(9):667–73. Available from: http://www.scielo.br/scielo.php?script=sci_arttext&pid=S0004-282X2012000900004&lng=en&nrm=iso&tlng=en

15. Cercignani M, Horsfield MA. The physical basis of diffusion-weighted MRI. J Neurol Sci . 2001 May 1;186 Suppl :S11–4. Available from: http://www.ncbi.nlm.nih.gov/pubmed/11334985

16. Westbrook C. MRI at a Glance. In: 3nd ed. Philadelphia, USA: Lippincott

Williams & Wilkins; 2002. p. p.12–20.

17. Johansen-Berg H, Behrens T. Diffusion MRI . 1st ed. Diffusion MRI. Amesterdam: Academic Press; 2009. 333-351 p. Available from: http://www.sciencedirect.com/science/article/pii/B9780123747099000158

18. O'Donnell LJ, Westin C-F. An introduction to diffusion tensor image analysis. Neurosurg Clin N Am . 2011 Apr;22(2):185–96, viii. Available from: http://www.pubmedcentral.nih.gov/articlerender.fcgi?artid=3163395&tool=pmcentrez&rendertype=abstract

19. Hasan KM, Walimuni IS, Abid H, Hahn KR. A review of diffusion tensor magnetic resonance imaging computational methods and software tools. Comput Biol Med . 2011 Dec;41(12):1062–72. Available from: http://www.pubmedcentral.nih.gov/articlerender.fcgi?artid=3135778&tool=pmcentrez&rendertype=abstract

20. Gigandet X. Global brain connectivity analysis by diffusion MR tractography. EPFL; 2009; Available from: http://infoscience.epfl.ch/record/140995

21. Sousa JMS. Análise da conectividade estrutural na doença de Parkinson . Faculdade de Ciências e Tecnologia; 2013. Available from: http://run.unl.pt//handle/10362/10918

22. Ticló AJ. Análise da evolução da conectividade estrutural em doentes de Parkinson . 2015. Available from: http://run.unl.pt//handle/10362/15586

23. Taylor PA, Cho K-H, Lin C-P, Biswal BB. Improving DTI tractography by including diagonal tract propagation. PLoS One . Public Library of Science; 2012 Jan;7(9):e43415. Available from: http://journals.plos.org/plosone/article?id=10.1371/journal.pone.0043415

24. Ferra CS. Conectividade estrutural do cérebro. Lisbon: Escola Superior de Tecnologia da Saúde de Lisboa; 2012. Available from: http://repositorio.ipl.pt//handle/10400.21/1733

25. Rubinov M, Sporns O. Complex network measures of brain connectivity: uses and interpretations. Neuroimage. 2010 Sep;52(3):1059–69. Available from: http://www.ncbi.nlm.nih.gov/pubmed/19819337

26. Menke RA, Jbabdi S, Miller KL, Matthews PM, Zarei M. Connectivity-based segmentation of the substantia nigra in human and its implications in

Parkinson’s disease. Neuroimage. 2010 Oct 1;52(4):1175–80. Available from: http://www.sciencedirect.com/science/article/pii/S1053811910008426

27. Friston KJ. Functional and effective connectivity: a review. Brain Connect . Mary Ann Liebert, Inc. 140 Huguenot Street, 3rd Floor New Rochelle, NY 10801 USA; 2011 Jan 1;1(1):13–36. Available from: http://online.liebertpub.com/doi/abs/10.1089/brain.2011.0008

28. Bondy A, Murty R. Graph theory. 1st ed. New York: Springer; 2011. 1-242 p.

29. Cochrane CJ, Ebmeier KP. Diffusion tensor imaging in parkinsonian syndromes: a systematic review and meta-analysis. Neurology. 2013 Feb 26;80(9):857–64. Available from: http://www.pubmedcentral.nih.gov/articlerender.fcgi?artid=3598454&tool=pmcentrez&rendertype=abstract

30. Baradaran N, Tan SN, Liu A, Ashoori A, Palmer SJ, Wang ZJ, et al. Parkinson’s disease rigidity: relation to brain connectivity and motor performance. Front Neurol. 2013 Jan;4:67. Available from: http://www.pubmedcentral.nih.gov/articlerender.fcgi?artid=3672800&tool=pmcentrez&rendertype=abstract

31. Agosta F, Caso F, Stankovic I, Inuggi A, Petrovic I, Svetel M, et al. Cortico-striatal-thalamic network functional connectivity in hemiparkinsonism. Neurobiol Aging. 2014 Nov;35(11):2592–602. Available from: http://www.ncbi.nlm.nih.gov/pubmed/25004890

32. Eickhoff SB, Grefkes C. Approaches for the integrated analysis of structure, function and connectivity of the human brain. Clin EEG Neurosci. 2011 Apr;42(2):107–21. Available from: http://www.ncbi.nlm.nih.gov/pubmed/21675600

33. Hacker CD, Perlmutter JS, Criswell SR, Ances BM, Snyder AZ. Resting state functional connectivity of the striatum in Parkinson’s disease. Brain. 2012 Dec 1;135(Pt 12):3699–711. Available from: http://brain.oxfordjournals.org/content/135/12/3699

34. Rieckmann A, Gomperts SN, Johnson KA, Growdon JH, Van Dijk KRA. Putamen-midbrain functional connectivity is related to striatal dopamine transporter availability in patients with Lewy body diseases. NeuroImage Clin. 2015 Jan;8:554–9. Available from:

http://www.sciencedirect.com/science/article/pii/S2213158215001072

35. Prakash BD, Sitoh Y-Y, Tan LCS, Au WL. Asymmetrical diffusion tensor imaging indices of the rostral substantia nigra in Parkinson's disease. Parkinsonism Relat Disord. 2012 Nov;18(9):1029–33. Available from: http://www.ncbi.nlm.nih.gov/pubmed/22705126

36. Scherfler C, Esterhammer R, Nocker M, Mahlknecht P, Stockner H, Warwitz B, et al. Correlation of dopaminergic terminal dysfunction and microstructural abnormalities of the basal ganglia and the olfactory tract in Parkinson's disease. Brain. 2013 Oct;136(Pt 10):3028–37. Available from: http://www.ncbi.nlm.nih.gov/pubmed/24014521

37. Yoshikawa K. Early pathological changes in the parkinsonian brain demonstrated by diffusion tensor MRI. J Neurol Neurosurg Psychiatry. 2004 Mar 1;75(3):481–4. Available from: http://jnnp.bmj.com/content/75/3/481

38. Batista K, Rodríguez R, Carballo M, Morales J. VI Latin American Congress on Biomedical Engineering CLAIB 2014, Paraná, Argentina 29, 30 & 31 October 2014. Braidot A, Hadad A, editors. Cham: Springer International Publishing; 2015. 397-400 p. Available from: http://link.springer.com/10.1007/978-3-319-13117-7

39. Ribeiro AS, Lacerda LM, da Silva NA, Ferreira HA. Multimodal imaging brain connectivity analysis (MIBCA) toolbox: preliminary application to Alzheimer's disease. EJNMMI Phys. 2014 Jul;1(Suppl 1):A61. Available from: http://www.pubmedcentral.nih.gov/articlerender.fcgi?artid=4545458&tool=pmcentrez&rendertype=abstract

40. Ribeiro AS, Lacerda LM, Ferreira HA. Multimodal Imaging Brain Connectivity Analysis toolbox (MIBCA). PeerJ Inc.; 2014 Dec 16; Available from: https://peerj.com/preprints/699v1

41. Tessitore A, Giordano A, Russo A, Tedeschi G. Structural connectivity in Parkinson's disease. Park Relat Disord. 2015;22.

42. Yoo K, Chung SJ, Kim HS, Choung O-H, Lee Y-B, Kim M-J, et al. Neural substrates of motor and non-motor symptoms in Parkinson's disease: a resting FMRI study. PLoS One. Public Library of Science; 2015 Jan;10(4):e0125455. Available from: http://journals.plos.org/plosone/article?id=10.1371/journal.pone.0125455

43. Pirogovsky-Turk E, Filoteo JV, Litvan I, Harrington DL. Structural MRI Correlates of Episodic Memory Processes in Parkinson's Disease Without Mild Cognitive Impairment. J Parkinsons Dis. IOS Press; 2015 Nov 21;5(4):971–81. Available from: http://content.iospress.com/articles/journal-of-parkinsons-disease/jpd150652

44. Aarabi MH, Kamalian A, Mohajer B, Shandiz MS, Eqlimi E, Shojaei A, et al. A statistical approach in human brain connectome of Parkinson Disease in elderly people using Network Based Statistics. Conf Proc . Annu Int Conf IEEE Eng Med Biol Soc IEEE Eng Med Biol Soc Annu Conf. IEEE; 2015 Aug;2015:4310–3. Available from: http://ieeexplore.ieee.org/articleDetails.jsp?arnumber=7319348

45. Meijer FJA, van Rumund A, Tuladhar AM, Aerts MB, Titulaer I, Esselink RAJ, et al. Conventional 3T brain MRI and diffusion tensor imaging in the diagnostic workup of early stage parkinsonism. Neuroradiology. 2015 Jul;57(7):655–69. Available from: http://www.pubmedcentral.nih.gov/articlerender.fcgi?artid=4495265&tool=pmcentrez&rendertype=abstract

46. Lucas-Neto L, Reimão S, Oliveira E, Rainha-Campos A, Sousa J, Nunes RG, et al. Advanced MR Imaging of the Human Nucleus Accumbens--Additional Guiding Tool for Deep Brain Stimulation. Neuromodulation. 2015 Jul;18(5):341–8. Available from: http://www.ncbi.nlm.nih.gov/pubmed/25879622

47. Mavridis IN. Is nucleus accumbens atrophy correlated with cognitive symptoms of Parkinson's disease? Brain. Oxford University Press; 2015 Jan 1;138(Pt 1):e319. Available from: http://brain.oxfordjournals.org/content/138/1/e319.abstract

48. O'Callaghan C, Hornberger M, Balsters JH, Halliday GM, Lewis SJG, Shine JM. Cerebellar atrophy in Parkinson's disease and its implication for network connectivity. Brain. 2016 Jan 20;awv399 – . Available from: http://brain.oxfordjournals.org/content/early/2016/01/20/brain.awv399.abstract

49. Mirdamadi JL. Cerebellar Role in Parkinson's Disease. J Neurophysiol. 2016 Jan 20;jn.01132.2015. Available from: http://jn.physiology.org/content/early/2016/01/15/jn.01132.2015

50. Anders S, Sack B, Pohl A, Münte T, Pramstaller P, Klein C, et al. Compensatory premotor activity during affective face processing in subclinical carriers of a single mutant Parkin allele. Brain. 2012 Apr 1;135(Pt 4):1128–40. Available from: http://brain.oxfordjournals.org/content/135/4/1128.short

51. Pellicano C, Assogna F, Piras F, Caltagirone C, Pontieri FE, Spalletta G. Regional cortical thickness and cognitive functions in non-demented Parkinson's disease patients: a pilot study. Eur J Neurol. 2012 Jan;19(1):172–5. Available from: http://www.ncbi.nlm.nih.gov/pubmed/21771199

52. Bertrand J-A, McIntosh R, Postuma RB, Kovacevic N, Latreille V, Panisset M, et al. Brain connectivity alterations are associated with dementia in Parkinson's disease. Brain Connect. 2015 Dec 28; Available from: http://online.liebertpub.com/doi/abs/10.1089/brain.2015.0390

53. Vervoort G, Alaerts K, Bengevoord A, Nackaerts E, Heremans E, Vandenberghe W, et al. Functional connectivity alterations in the motor and fronto-parietal network relate to behavioral heterogeneity in Parkinson's disease. Parkinsonism Relat Disord. Elsevier Science; 2016 Jan 1; Available from: https://lirias.kuleuven.be/handle/123456789/523566

54. Pagonabarraga J, Corcuera-Solano I, Vives-Gilabert Y, Llebaria G, García-Sánchez C, Pascual-Sedano B, et al. Pattern of regional cortical thinning associated with cognitive deterioration in Parkinson's disease. PLoS One. 2013 Jan;8(1):e54980. Available from: http://www.pubmedcentral.nih.gov/articlerender.fcgi?artid=3554657&tool=pmcentrez&rendertype=abstract

Appendix A

Sample characterization

Control (0); SWEDD (1) – Scans Without Evidence for Dopaminergic Deficit; PD (2) – Parkinson's Disease; YrsEdu – Years of education in years; Age – years old; UPDRS – Unified Parkinson's Disease Rating Scale; Feminine (0) –; Masculine (1) –.

Number	Patient ID	Group	Gender	Age	YrsEdu	UPDRS
1	3106	0	0	70	13	0
2	3112	0	0	63	16	0
3	3114	0	0	64	21	1
4	3115	0	1	61	16	0
5	3151	0	1	58	13	2
6	3157	0	0	64	20	3
7	3171	0	1	61	16	3
8	3161	0	1	45	16	8
9	3165	0	0	59	16	3
10	3169	0	1	57	14	5
11	3191	0	0	66	18	3
12	3300	0	1	52	18	2
13	3301	0	1	52	20	1
14	3310	0	1	65	16	7
15	3316	0	1	75	22	2
16	3320	0	1	56	20	1
17	3389	0	1	72	16	3
18	3390	0	1	66	17	5
19	3188	0	1	71	18	2
20	3172	0	1	70	17	3
21	3554	0	1	75	18	2
22	3555	0	1	40	11	13
23	3563	0	1	60	16	2
24	3569	0	0	40	13	1
25	3570	0	1	72	18	2
26	3571	0	1	46	18	1
27	3572	0	0	58	16	0
28	3750	0	1	53	17	0
29	3756	0	1	65	12	8
30	3759	0	0	54	16	0
31	3101	1	1	50	23	12
32	3170	1	0	60	19	11
33	3183	1	1	64	18	15
34	3189	1	0	71	18	15
35	3580	1	0	69	16	45

36	3324	1	1	55	20	37
37	3326	1	1	69	24	12
38	3550	1	0	51	12	25
39	3566	1	0	50	16	7
40	3573	1	1	52	14	47
41	3580	1	0	69	16	45
42	3581	1	1	53	14	24
43	3582	1	0	63	21	27
44	3751	1	1	53	10	21
45	3783	1	0	52	19	14
46	3810	1	1	67	12	24
47	3820	1	1	77	8	7
48	3821	1	1	67	8	48
49	3836	1	0	59	9	49
50	3860	1	0	47	9	38
51	3861	1	1	69	9	25
52	3862	1	1	62	11	46
53	3865	1	1	77	8	18
54	4023	1	0	63	24	64
55	4031	1	0	62	15	26
56	4036	1	0	50	16	17
57	4060	1	1	80	19	21
58	4064	1	1	73	16	15
59	4066	1	1	61	24	23
60	4084	1	1	59	17	12
61	3102	2	1	64	16	36
62	3105	2	1	69	18	44
63	3107	2	1	70	16	24
64	3108	2	0	50	18	29
65	3111	2	1	65	14	34
66	3116	2	1	65	18	70
67	3118	2	1	60	14	26
68	3119	2	1	64	16	38
69	3120	2	0	50	18	38
70	3122	2	1	62	16	25
71	3123	2	1	69	18	16
72	3124	2	1	57	16	29
73	3125	2	1	46	16	28
74	3126	2	1	64	18	35
75	3127	2	0	49	16	16
76	3128	2	0	60	18	25
77	3129	2	1	56	16	41
78	3130	2	1	44	18	13
79	3132	2	1	50	16	27

80	3167	2	0	59	14	38
81	3168	2	0	63	16	42
82	3173	2	0	62	18	20
83	3174	2	1	51	18	26
84	3175	2	0	57	20	17
85	3176	2	1	62	19	17
86	3178	2	1	72	18	6
87	3181	2	0	65	14	32
88	3182	2	0	55	18	44

Appendix B

Statistical analysis of structural brain connectivity

Divulges main significant regional increases and decreases in connectivity metrics between the second and first groups. Regions with 2, 3 and 4 significant changes are exhibited in bold, underlined, and italic, correspondingly. No CAr decreases were observed.

	Control-PD	Control-SWEDD	SWEDD-PD
CThk increase	**Rh**-PHG, FG, **caCG**; **Lh**-ERC		**Rh**-FP, rMFG, **Lh**-FP
CThk decrease		**Rh-FP**; **Lh-parsO**	
CAr increase	**Rh**-SFG, PCn, parsT, **ERC**, Cn; **Lh**-Ins, TP, SFG, parsO, FG	**Lh-SPG, parsO**	**Rh**-PCn, MTG, **iCG**, **Cn**; **Lh**-FG
CVol increase	**Rh**-Ins, pCG; **Lh**-PHG	**Rh**-Ins	**Rh**-FP, SFG, rMFG, PHG, ITG; **Lh**-FP, **SFG**, PHG, ITG,
CVol decrease		**Rh-FP**	
FA increase	R-Acc, CCp	**Rh-SMG**, SPG, PoCG, **iCG**; **Lh**-Ins, **SMG**, **SPG**, PoCG, PaCG, **iCG**, **Bankssts**, **R-Pd**, **CCp**	
FA decrease	**Rh**-FP, rMFG, parsT, parsO, **ERC**, **caCG**; **Lh**-FP, rMFG, **parsT**, parsO, parsOp, caMCG		**Rh-Ins**, SMG, SPG, rMFG, PCG, PoCG, parsT, **parsO**, ParsOp, PHG, LOFG, IPL, **ERC**, **Cn**, Bankssts; **Lh-Ins**, **TTG,** FP, SMG, STG, **SFG**, **rMFG**, **PCG**, PoCG, **parsT**, parsO, parsOp, PHG, iCG, Bankssts
MD increase	**Rh**-FP, rMFG, parsT;		**Rh-Ins**, **parsO**, PHG, MeOFC, LOFG, **ICG**

	Lh-rMFG, **parsT**, parsO		**ERC**, Bankssts; **Lh-Ins**, **parsT**, parsO, PHG, ERC
MD decrease	R-Acc, R-Cerbll: L- Pd, L-Cerbll, CCc, CCmpo	**Rh**-Ins, **SMG**, **parsO**, MeOFC, LG**, iCG**; **Lh**-Ins, **SMG**, **iCG**, ITG, **Bankssts**, L-Pd, **CCp**; **R-Pd**, **R-Cerbll**	
ClusC increase		**Rh**-Ins, PCn; **Lh**-Ins, SFG	**Lh-SPG**
ClusC decrease	L-Cerbll	**Lh**-PCG	**L-Cerbll**, **PCG**
Deg increase		**Rh**-rMFG, raCG	**L-Cerbll**
Deg decrease		**R-Cerbll**	**Rh**-LG, LOFG, **LOG**; **Lh-TTG**, FP, **SPG**, **rMFG**, parsO, CCp
Betw increase	**Rh**-SMG, L-Cerbll		
Betw decrease	**Lh**-parsO	**Rh**-Bankssts, **parsO**, IPG	**Rh**-Bankssts; **Lh**-parsO, IPL
FiberConn	Decrease highlight in subcortical regions: Between R-Thal and **Rh**-FP and rMFG; R-Pt and **Rh**-SFG, R-Hip and **Rh**-PCG, **Lh**-Pt and **Lh**-LOFG and **Lh**-TTG; Decrease Highlight in connections in cortical regions: **Rh**-PCn, **Lh**-LOG, **Lh**-PaCG, **Lh**-SPG, **Rh**-LOG and **Rh**-ITG; **Lh**-Ins, **Lh**-TP, **Lh**-parsO, **Lh**-LOFG, **Lh**-PCn, **Lh**-LOF and **Lh**-rMFG Increase highlight in subcortical and Cortical regions: R-Caudate,	Decrease highlight in connection in **Lh**-SPG, PoCG, **Lh**-Tha, **Rh**-Acc and Pd. Increase highlight: **Rh**-SPG, **Rh**-LOFG, **Rh**-Tha, CCp and **Lh**-LOFG.	Bilateral hemisphere decreasing. Decreasing in connections with R-Hip Increasing connections between L-Acc with another **Lh** structures: Tp, and Ins, and increasing connections with R and L-Cerebll

	CCp, CCa; Fp, **Rh**-PCn, **Rh**-parsO, LOG, R-Acc and **Lh**-PHG		
Dist	General increase of distance connections, especially in occipital and temporal regions	General decrease of distance connections in both hemispheres	General increase of distance connections, regarding subcortical regions: L-Cd, L-Hip, R-Tha and R-Cerebll
Edge Betw	Decrease highlight: **Rh**-Ins, **Lh**-ITG Increase Highlight: R-Acc	Decrease highlight: **Rh**-parsT.	Decrease highlight: **Rh**-STG, LOFG Increase Highlight: R-Cd, **Rh**-PCn, PoCG

Appendix C

Statistical differences values of all metrics obtained with MIBCA software

Statistics differences values of all metrics obtained with MIBCA software for the comparison between Control vs PD, regarding the T1, DTI and connectivity metrics. Red and Blue squares, respectively represent, lower and higher values for the second group in comparison to the first. The brain regions that hadn't presented any results were automatic excluded.

	CThk (mm)	Car (mm2)	Cvol (mm3)	FA	MD	ClustC	Deg	Betw
FP				**Lh**: 0.37-0.46 **Rh**: 0.36-0.44	**Rh**: 4.27e-04-3.32e-04			
SMG								**Rh**: 178.46-104.46
LG							**Rh**: 6.43-6.83	
FG	**Rh**: 3.24-3.20	**Rh**: 0.62-0.61						
TP		**Lh**: 0.64-0.61						
rMFG				**Rh**: 0.45-0.49	**Lh**: 4.03e-04-3.62e-04 **Rh**: 3.69e-04-3.41e-04			
SFG		**Lh**: 0.62-0.61						
caCG	**Rh**: 2.90-2.75			**Rh**: 0.48-0.51				
pCG			**Rh**: 2.01-1.95					
caMFG				**Lh**: 0.44-0.48				
PHG	**Rh**: 3.16-2.98		**Lh**: 2.45-2.27				**Rh**: 9.87-11.7	
ParsO		**Rh**: 0.60-0.59		**Lh**: 0.51-0.55 ; **Rh**: 0.53-0.58	**Lh**: 2.92e-04-2.62e-04			**Lh**: 80.57-196.65
ParsT		**Rh**: 0.63-0.61		**Lh**: 0.47- ; **Rh**:0.49-	**Lh**: 3.41e-04-3.04e-04; **Rh**: 3.24e-04-2.97e-04			
ParsOp				**Lh**: 0.47-0.51				
ERC	**Lh**: 3.80-3.66	**Rh**: 0.62-0.60		**Rh**: 0.54-0.59				
Acc				**Rh**: 0.76-0.70	**Rh**: 2.08e-04-2.45e-04			
CCp				1.08-1.05				
CCmp					3.35e-04-3.71e-04			
CCc					3.12e-04-3.35e-04			
Pd					**L**: 1.75e-04-1.96e-04			
Ins		**Lh**: 0.65-0.63	2.27-2.20					
Cn		**Rh**: 0.57-0.54						
PCn		**R**: 0.62-0.61						

	CThk (mm)	Car (mm^2)	Cvol (mm^3)	FA	MD	ClustC	Deg	Betw
PCG							**Lh**: 24.79-23	
CerebII					**L**: 2.38e-04-2.51e-04; **R**: 2.15e-04-2.35e-04	**L**: 26.38-30.00		**L**: 264.32-135.76

Statistics differences values of all metrics obtained with MIBCA software for the comparison between Control vs SWEDD, regarding the T1, DTI and connectivity metrics. Red and Blue squares, respectively represent, lower and higher values for the second group in comparison to the first. The brain regions that hadn't presented any results were automatic excluded.

	CThk (mm)	Car (mm^2)	Cvol (mm3)	FA	MD	ClustC	Deg	Betw
FP	**Rh**: 2.81-3,03		**Rh**: 2,25-2,55					
ITG					**Lh**: 2.24e-04-3,02e-04			
MTG								
STG								
TTG								
SMG				**Lh**: 0,46-0,41; **Rh**: 0,46-0,41	**Lh**: 3.01e-04-3.96e-04; **Rh**: 3.04e-04-4.04e-04			
SPL		**Lh**: 0.62-0.62		**Lh**: 0.47-0.43; **Rh**: 0.49-0.44				
IPL								
LG					**Rh**: 3.20e-04-4.17e-04			**Rh**: 413.16-237.75
FG								
TP								
MeOFC					**Rh**: 3.19e-04-4.28e-04			
rMFG							**Lh**: 19.87-16.97	
SFG						**Lh**: 23.95-20.54		
iCG				**Lh**: 0.58-0.52; **Rh**: 0.60-0.53	**Lh**: 2.87e-04-3.95e-04; **Rh**: 2.80e-04-3.91e-04			
caCG								
raCG							**Lh**: 13.17-11.76	
ParsO	**Lh**: 3.04-3.19	**Lh**: 0.60-0.59			**Rh**: 2.79e-04-3.68e-04			
CCp					2.93e-04-3.81e-04			
CCmp								
Pd					**L**: 2.96e-04-4.07e-04; **R**: 2.08e-04-2.75e-04			
Ins			**Rh**: 2.27-2.17	**Lh**: 0.56-0.50	**Lh**: 2.74e-04-3.73e-04; **Rh**: 2.82e-04-4.01e-04	**Lh**: 15.83-14.01; **Rh**: 13.90-12.54		
Cn								

PCn						**Rh**: 15.32-13.07		
PaCG				**Lh**: 0.50-0.43				
PoCG				**Lh**: 0.46-0.41; **Rh**: 0.45-0.40				**Rh**: 307.99-202.93
Bankssts				**Lh**: 0.48-0.42	**Lh**: 2.50e-04-3.41e-04			
CerebII					**R**: 2.15e-04-3.02e-04		**R**: 16.23-18.10	

Statistics differences values of all metrics obtained with MIBCA software for the comparison between SWEDD VS PD, regarding the T1, DTI and connectivity metrics. Red and Blue squares, respectively represent, lower and higher values for the second group in comparison to the first. The brain regions that hadn't presented any results were automatic excluded.

	CThk (mm)	**Car (mm^2)**	**Cvol (mm3)**	**FA**	**MD**	**ClustC**	**Deg**	**Betw**
FP	**Lh**: 3.08-2.90; **Rh**: 3.03-2.72		**Lh**: 2.72-2.36; **Rh**: 2.75-2.14	**Lh**: 0.36-0.46			**Lh**: 10.55-13.24	
ITG			**Lh**: 2.44-2.32; **Rh**: 2.47-2.35	**Rh**: 0.43-0.50				
MTG		**Rh**: 0.63-0.62						
STG				**Lh**: 0.43-0.48				
TTG				**Lh**: 0.44-0.51			**Lh**: 5.76-6.59	
SMG				**Lh**: 0.41-0.47; **Rh**: 0.41-0.47				
SPL				**Rh**: 0.44-0.51		**Lh**: 20.54-17.93	**Lh**: 24.93-28.38	
IPL								**Lh**: 105.68-272.66
LG							**Rh**: 18.69-21.21	
FG		**Lh**: 0.63-0.62						
MeOFC					**Rh**: 4.28e-04-3.17e-04			
rMFG	**Rh**: 2.80-2.68		**Rh**: 1.88-2.00	**Lh**: 0.39-0.46; **Rh**: 0.43-0.49			**Lh**: 16.97-21.79	
SFG			**Lh**: 2.16-2.27; **Rh**: 2.07-2.17					

LOFG				**Rh**: 0.51-0.59	**Rh**: 3.47e-04-2.47e-04		**Lh**: 17.10-21.76; **Rh**: 18.66-21.76	
LOG							**Rh**: 16.62-19.24	
iCG		**Rh**: 0.60-0.59		**Lh**: 0.52-0.58	**Rh**: 3.91e-04-2.94e-04			
pCG						**Rh**: 13.61-15.49		
PHG			**Lh**: 2.27-2.46; **Rh**: 2.16-2.34	**Lh**: 0.53-0.62; **Rh**: 0.52-0.63	**Lh**: 4.08e-04-2.84e-04; **Rh**: 4.01e-04-2.79e-04			
ParsO				**Lh**: 0.47-0.55; **Rh**: 0.48-0.58	**Lh**: 3.74e-04-2.73e-04; **Rh**: 3.68e-04-2.66e-04		**Lh**: 8.69-10.69	**Lh**: 66.34-196.65
ParsT				**Lh**: 0.45-0.52; **Rh**: 0.46-0.53	**Lh**: 4.05e-04-3.05e-04			
ParsOp				**Lh**: 0.45-0.51; **Rh**: 0.44-0.51				
ERC				**Lh**: 4.63e-04-3.04e-04; **Rh**: 0.49-0.59	**Rh**: 4.29e-04-2.99e-04			
CCp							13.28-16.10	
Ins				**Lh**: 0.50-0.58; **Rh**: 0.50-0.57	**Lh**: 3.73e-04-2.77e-04; **Rh**: 4.01e-04-2.84e-04			
Cn		**Rh**: 0.56-0.54		0.40-0.47				
PCn		**Rh**: 0.62-0.61						

	CThk (mm)	Car (mm^2)	Cvol (mm3)	FA	MD	ClustC	Deg	Betw
PCG				**Lh**: 0.44-0.50; **Rh**: 0.44-0.49				
PoCG				**Lh**: 0.41-0.46; **Rh**: 0.40-0.46				
Bankssts				**Lh**: 0.42-0.49; **Rh**: 0.43-0.51				**Rh**: 3.69-40.54
Cerebll						L: 25.00-30.00	L: 18.17-16.45	

Appendix D

Control vs PD Connectogram

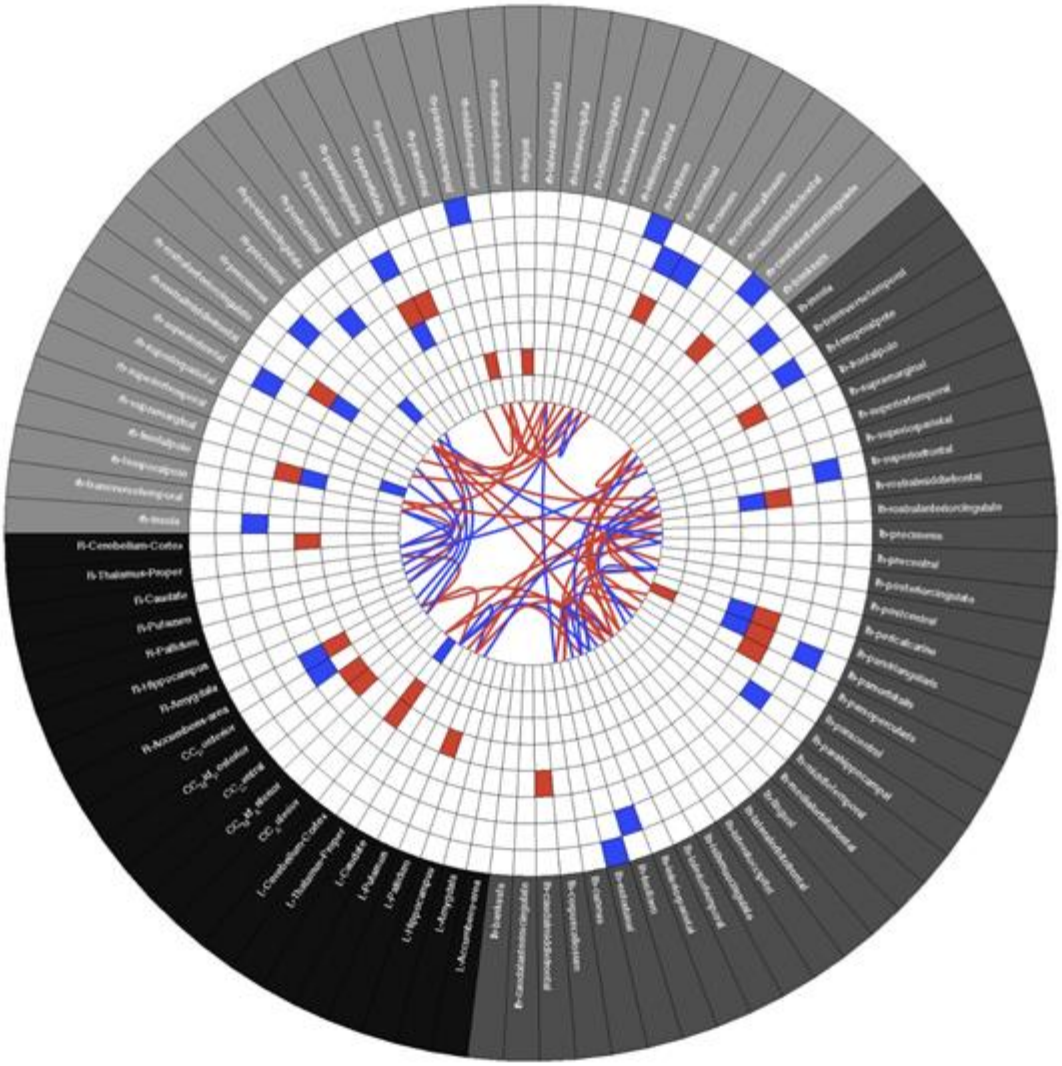

Connectogram for CONTROL vs PD. Right (Rh) and left (Lh) hemisphere represent the cortical brain regions (R-light gray and L darker gray) and the black regions characterises subcortical regions. From inner to outer rings the sequence used were: cortical thickness, cortical area, cortical and subcortical volumes volume fractional anisotropy, mean diffusivity, clustering coefficient, node degree and betweeness centrality. Red and Blue squares, respectively represent, lower and higher values of the conforming ring metric for the second group in comparison to the first. In the centre we have the structural diffusion tensor imaging connectivity data, where Red and Blue lines, respectively represent, decreasing and increasing number of fiber between the groups.

Appendix E

Control vs SWEDD Connectogram

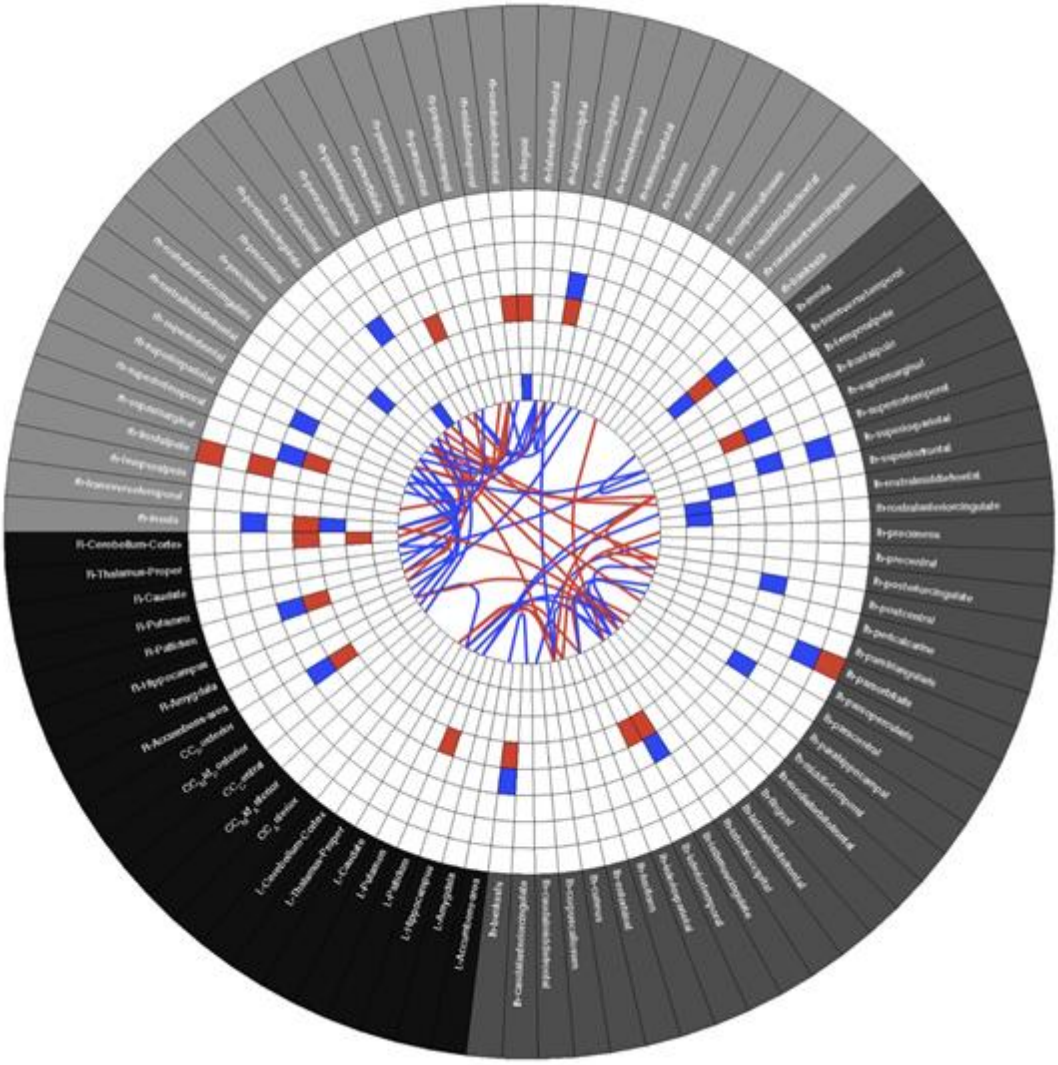

Connectogram for CONTROL-SWEDD. Right (Rh) and left (Lh) hemisphere represent the cortical brain regions (R-light gray and L darker gray) and the black regions characterises subcortical regions. From inner to outer rings the sequence used were: cortical thickness, cortical area, cortical and subcortical volumes volume fractional anisotropy, mean diffusivity, clustering coefficient, node degree and betweeness centrality. Red and Blue squares, respectively represent, lower and higher values of the conforming ring metric for the second group in comparison to the first. In the centre we have the structural diffusion tensor imaging connectivity data, where Red and Blue lines, respectively represent, decreasing and increasing number of fiber between the groups.

Appendix F

SWEDD vs PD Connectogram

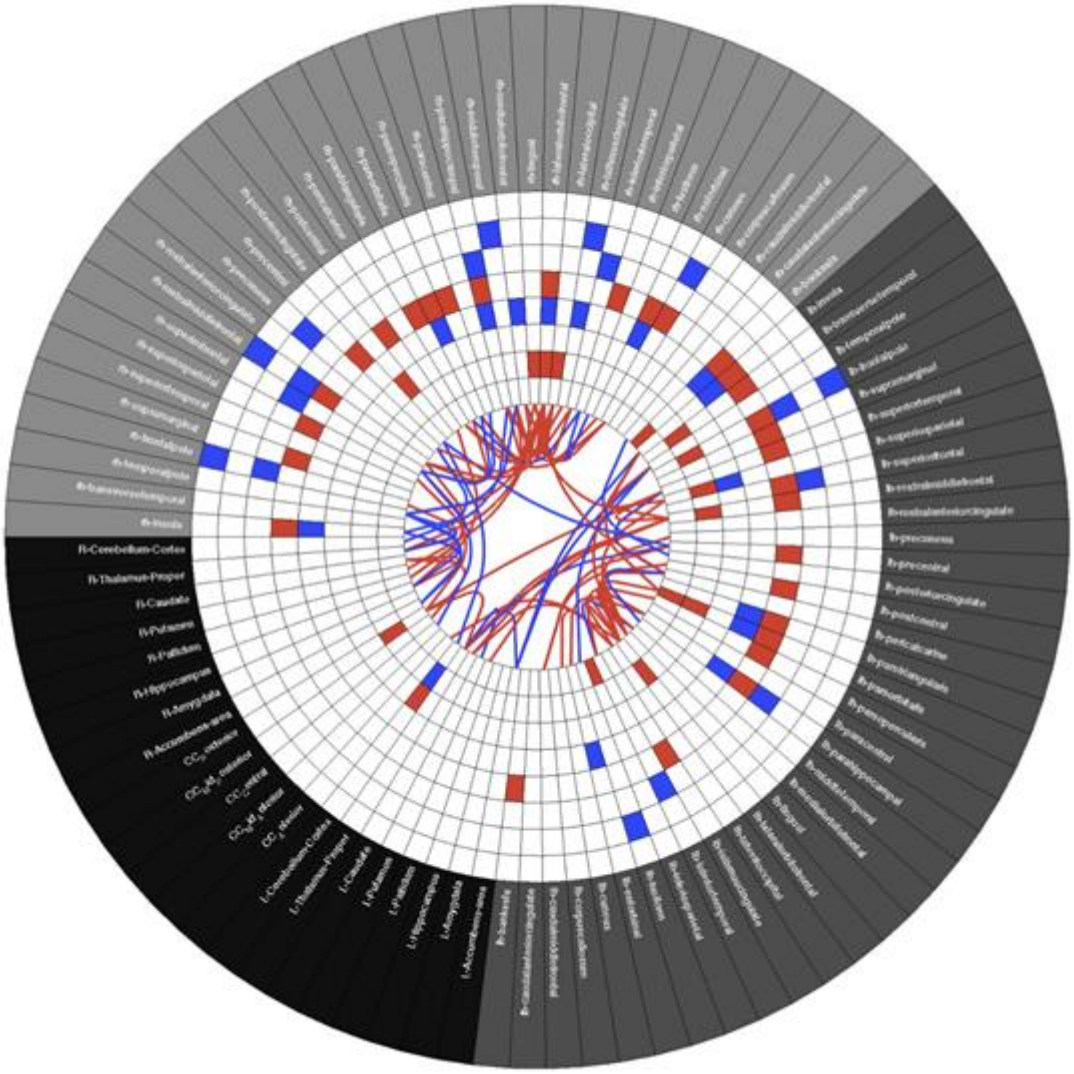

Connectogram for SWEDD-PD. Right (Rh) and left (Lh) hemisphere represent the cortical brain regions (R-light gray and L darker gray) and the black regions characterises subcortical regions. From inner to outer rings the sequence used were: cortical thickness, cortical area, cortical and subcortical volumes volume fractional anisotropy, mean diffusivity, clustering coefficient, node degree and betweeness centrality. Red and Blue squares, respectively represent, lower and higher values of the conforming ring metric for the second group in comparison to the first. In the centre we have the structural diffusion tensor imaging connectivity data, where Red and Blue lines, respectively represent, decreasing and increasing number of fiber between the groups.

Appendix E

National and international communications related with this research

---

2016: Constantino T, Maximiano R, Santos-Ribeiro A, McGonigle J, Nutt D, Ferreira H, “Brain Connectivity Analysis of Parkinson's Disease and "Scans Without Evidence for Dopaminergic Deficit" Patients”, ISMRM 2016 - 24th Annual Meeting, 7-13 May 2016, Singapore (e-poster).

2016: Maximiano R, Constantino T, Santos-Ribeiro A, Ferreira H. “Automatic Classification of Brain Connectivity Matrix - a toolbox for supporting neuropsychiatric diagnosis”, ISMRM 2016 - 24th Annual Meeting, 7-13th May 2016, Singapore.

2015: Maximiano R, Constantino T, Santos-Ribeiro A, Ferreira H. Automatic Classification of Brain Connectivity Matrix – a toolbox for supporting neuropsychiatric diagnosis. 1o Encontro de Alunos de Doutoramento do Colégio Mente-Cérebro da Universidade de Lisboa, 20th December 2015. Universidade de Ciências de Lisboa. Traditional Poster.